

Detecting the Yarkovsky effect among near-Earth asteroids from astrometric data

Alessio Del Vigna^{a,b}, Laura Faggioli^d, Andrea Milani^a, Federica Spoto^c,
Davide Farnocchia^e, Benoit Carry^f

^a*Dipartimento di Matematica, Università di Pisa, Largo Bruno Pontecorvo 5, Pisa, Italy*

^b*Space Dynamics Services s.r.l., via Mario Giuntini, Navacchio di Cascina, Pisa, Italy*

^c*IMCCE, Observatoire de Paris, PSL Research University, CNRS, Sorbonne University, UPMC Univ. Paris 06, Univ. Lille, 77 av. Denfert-Rochereau F-75014 Paris, France*

^d*ESA SSA-NEO Coordination Centre, Largo Galileo Galilei, 1, 00044 Frascati (RM), Italy*

^e*Jet Propulsion Laboratory/California Institute of Technology, 4800 Oak Grove Drive, Pasadena, 91109 CA, USA*

^f*Université Côte d'Azur, Observatoire de la Côte d'Azur, CNRS, Laboratoire Lagrange, Boulevard de l'Observatoire, Nice, France*

Abstract

We present an updated set of near-Earth asteroids with a Yarkovsky-related semi-major axis drift detected from the orbital fit to the astrometry. We find 87 reliable detections after filtering for the signal-to-noise ratio of the Yarkovsky drift estimate and making sure the estimate is compatible with the physical properties of the analyzed object. Furthermore, we find a list of 24 marginally significant detections, for which future astrometry could result in a Yarkovsky detection. A further outcome of the filtering procedure is a list of detections that we consider spurious because unrealistic or not explicable with the Yarkovsky effect. Among the smallest asteroids of our sample, we determined four detections of solar radiation pressure, in addition to the Yarkovsky effect. As the data volume increases in the near future, our goal is to develop methods to generate very long lists of asteroids with reliably detected Yarkovsky effect, with limited amounts of case by case specific adjustments. Furthermore, we discuss the improvements this work could bring to impact monitoring. In particular, we exhibit two asteroids for which the adoption of a non-gravitational model is needed to make reliable impact predictions.

Keywords: Asteroids, Yarkovsky effect, Non-gravitational perturbations, Orbit determination, Impact Monitoring

Email address: delvigna@mail.dm.unipi.it (Alessio Del Vigna)

1. Introduction

Several complex phenomena cause asteroid orbital evolution to be a difficult problem. By definition, Near-Earth Asteroids (NEAs) experience close approaches with terrestrial planets, which are the main source of chaos in their orbital evolution. Because of this chaoticity, small perturbations such as non-gravitational ones can significantly affect a NEA trajectory.

The *Yarkovsky effect* is due to the recoil force undergone by a rotating body as a consequence of its anisotropic thermal emission (Vokrouhlický et al., 2000, 2015a). The main manifestation of the Yarkovsky effect is a secular semimajor axis drift da/dt , which leads to a mean anomaly runoff that grows quadratically with time. Typical values of this perturbation for sub-kilometre NEAs are $da/dt \simeq 10^{-4}$ – 10^{-3} au/My. Because of its small size, the Yarkovsky effect can only be detected for asteroids with a well constrained orbit.

The Yarkovsky effect is a non-gravitational perturbation generally split into a seasonal and a diurnal component. The seasonal component arises from the temperature variations that the heliocentric asteroid experiences as a consequence of its orbital motion. An explicit computation of the corresponding acceleration is not easy, even for a spherical body, and becomes very difficult for complex shaped bodies. On the other hand, the diurnal component is due to the lag between the absorption of the radiation coming from the Sun, and the corresponding re-emission in the thermal wavelength. The surface of a rotating body illuminated by the Sun is warmed by solar radiation during the day and cools at night. It is worth noticing that the diurnal and the seasonal components have different consequences on the secular semimajor axis drift. In particular, the diurnal effect produces a positive drift for prograde rotators and a negative drift for retrograde rotators, whereas the seasonal secular drift is always negative. The magnitude of the diurnal effect is generally larger than that of the seasonal effect (Vokrouhlický et al., 2000).

The Yarkovsky effect is key to understanding several aspects of asteroids dynamics:

1. Non-gravitational forces can be relevant for a reliable impact risk assessment when in the presence of deep planetary encounters or when having a long time horizon for the potential impact search (Farnocchia et al., 2015b). As a matter of fact, both these factors call for a greater consideration of the sources of orbit propagation uncertainty, such as non-gravitational perturbations. Currently, there are four known cases that required the inclusion of the Yarkovsky effect in term of hazard

assessment: (101955) Bennu (Milani et al., 2009; Chesley et al., 2014), (99942) Apophis (Chesley, 2006; Giorgini et al., 2008; Vokrouhlický et al., 2015b; Farnocchia et al., 2013a), (29075) 1950 DA (Giorgini et al., 2002; Farnocchia and Chesley, 2014), and (410777) 2009 FD (Spoto et al., 2014).

2. The semimajor axis drift produced by the Yarkovsky effect has sculpted the main belt for millions of years (Vokrouhlický et al., 2006). The Yarkovsky effect is crucial in understanding the aging process of asteroid families and the transport mechanism from the main belt to the inner Solar System (Vokrouhlický et al., 2000). The Yarkovsky effect has still not been measured in the main belt, thus Spoto et al. (2015) used a calibration based on asteroid (101955) Bennu to compute the ages of more than 50 families in the main belt. The improvement in the detection of the Yarkovsky drift for NEAs represents a new step forward in creating a reliable chronology of the asteroid belt.
3. Yarkovsky detections provide constraints on asteroid physical properties. Two remarkable efforts in estimating the bulk density from the Yarkovsky drift have already been done for two potentially hazardous asteroids: (101955) Bennu (Chesley et al., 2014) and (29075) 1950 DA (Rozitis et al., 2014). Furthermore, the dependence of the Yarkovsky effect on the obliquity can be useful to model the spin axis obliquity distribution of near-Earth asteroids (Tardioli et al., 2017).

Several efforts have been done in modelling and determining the Yarkovsky effect on the NEA population. The first detection of the Yarkovsky effect was predicted for the asteroid (6489) Golevka in Vokrouhlický et al. (2000) and achieved in 2003 thanks to radar ranging of this object (Chesley et al., 2003). Later, the Yarkovsky effect played a fundamental role in the attribution of four 1953 precovery observations to the asteroid (152563) 1992 BF (Vokrouhlický et al., 2008). Moreover, Chesley et al. (2014) detected the Yarkovsky effect acting on (101955) Bennu from the astrometric observations and from high-quality radar measurements over three apparitions. Currently, asteroid Bennu has the best determined value for the Yarkovsky acceleration, which also led to an estimation of its bulk density (Chesley et al., 2014). More in general, Nugent et al. (2012) provided a list of 13 Yarkovsky detection, and later work increased this number to 21 (Farnocchia et al., 2013b). The most recent census is from Chesley et al. (2016), which identified 42 NEAs with valid Yarkovsky detection. Both Farnocchia et al. (2013b) and Chesley et al. (2016) flag spurious cases based on whether the detected drift is compatible with the physical properties of the correspond-

ing object and the Yarkovsky mechanism. Since the number of significant Yarkovsky detections in the NEA population is steadily increasing, we decided to update the list.

2. Method

2.1. Force model

Usually, there is not enough information on an asteroid’s physical model to directly compute the Yarkovsky acceleration through a thermophysical model. Instead, evidence of the Yarkovsky-related drift may be detectable from the observational dataset via orbit determination. Indeed, a gravity-only model may not provide a satisfactory fit to the available data. A Yarkovsky detection is more likely when a very accurate astrometric dataset is available, especially in case of radar measurements at multiple apparitions, or when the observational arc is long, thus allowing the orbital drift to become detectable. In such cases, a force model including also the Yarkovsky acceleration could result in a better fit to the observations.

We model the Yarkovsky perturbation with a formulation that depends on a single dynamical parameter, to be determined in the orbital fit together with the orbital elements. Since the secular perturbation caused by the Yarkovsky effect is a semimajor axis drift, we use a transverse acceleration

$$\mathbf{a}_t = A_2 g(r) \hat{\mathbf{t}} \quad (1)$$

as in Marsden et al. (1973) and Farnocchia et al. (2013b). In equation (1) A_2 is a free parameter and $g(r)$ is a suitable function of the heliocentric distance of the asteroid. In particular we assume a power law

$$g(r) = \left(\frac{r_0}{r}\right)^d,$$

where $r_0 = 1$ au is used as normalization factor. The exponent d depends on the asteroid and is related to the asteroid’s thermophysical properties. Farnocchia et al. (2013b) show that the value of d is always between 0.5 and 3.5. They used $d = 2$ for all asteroids because no thermophysical data are available. In our analysis we adopted the same values for d , apart from (101955) Bennu for which the value $d = 2.25$ is assumed (Chesley et al., 2014).

Typical values of the Yarkovsky acceleration for a sub-kilometre NEA are 10^{-15} – 10^{-13} au/d². As a consequence, to reliably estimate the Yarkovsky effect, the right-hand side of the equations of motion has to include all

the accelerations down to the same order of magnitude. Our force model includes the gravitational accelerations of the Sun, the eight planets, and the Moon based on JPL’s planetary ephemerides DE431 (Folkner et al., 2014). To ensure a more complete force model, we also include the contributions coming from 16 massive main belt bodies and Pluto. All the gravitational masses we used are listed in Table 1. Since we compare our results with the ones obtained by JPL, we point out that the JPL team uses the 16 most massive main belt asteroids as estimated by Folkner et al. (2014), which produces a slight difference, both in the list and in the masses.

Table 1: Perturbing bodies included in the dynamical model in addition to the Sun, the planets and the Moon. They are 16 massive main belt bodies and Pluto. The last column shows the references we used for each asteroid mass.

Asteroid	Grav. mass (km^3/s^2)	Reference
(1) Ceres	63.20	Standish and Hellings (1989)
(2) Pallas	14.30	Standish and Hellings (1989)
(3) Juno	1.98	Konopliv et al. (2011)
(4) Vesta	17.80	Standish and Hellings (1989)
(6) Hebe	0.93	Carry (2012)
(7) Iris	0.86	Carry (2012)
(10) Hygea	5.78	Baer et al. (2011)
(15) Eunomia	2.10	Carry (2012)
(16) Psyche	1.81	Carry (2012)
(29) Amphitrite	0.86	Carry (2012)
(52) Europa	1.59	Carry (2012)
(65) Cybele	0.91	Carry (2012)
(87) Sylvia	0.99	Carry (2012)
(88) Thisbe	1.02	Carry (2012)
(511) Davida	2.26	Carry (2012)
(704) Interamnia	2.19	Carry (2012)
(134340) Pluto	977.00	Folkner et al. (2014)

The relativity model includes the relativistic contribution of the Sun, the planets and the Moon. In particular, we use the Einstein-Infeld-Hoffman equations, namely the equations of the approximate dynamics of a system of point-like masses due to their mutual gravitational interactions, in a first order post-Newtonian expansion, as described in Einstein et al. (1938); Will (1993); Moyer (2003).

2.2. Statistical treatment of the astrometry

The statistical treatment of the astrometry is key to a reliable orbit determination. The differential corrections procedure provides the asteroid’s nominal orbit and its uncertainty (Milani and Gronchi, 2010, Chap. 5), which strongly depend upon the observations accuracy and error modelling. For the computations done for this paper, we used the debiasing and weighting scheme provided in Farnocchia et al. (2015a). The JPL team uses the more recent Vereš et al. (2017) weighting scheme.

The astrometric data usually can contain outliers that can affect the solution of the orbit determination. To remove erroneous observations from the fit we apply the outlier rejection procedure described in Carpino et al. (2003).

Besides our default data treatment, we applied *ad hoc* modifications for the following cases:

(152563) 1992 BF. The four 1953 precovery observations of this NEA have been carefully re-measured in Vokrouhlický et al. (2008). We adopt the given positions and standard deviations, the latter being 0.5 arcsec in right ascension and 1 arcsec in declination.

2009 BD. This object is one of the smallest near-Earth asteroids currently known (Mommert et al., 2014b) and thus solar radiation pressure affects its orbit. A direct detection of the area-to-mass ratio is contained in Micheli et al. (2012), which provide high-quality astrometry from Mauna Kea and replace all the observations from the Tzec Maun Observatory (H10) with a single position. For these observations we set data weights based on the uncertainties provided by Micheli et al. (2012) and we include both the Yarkovsky effect and solar radiation pressure in the orbital fit (see Section 6).

2011 MD. As well as 2009 BD, this asteroid is very small and is among those for which we determined both the Yarkovsky effect and solar radiation pressure. 2011 MD has been observed during the 2011 very close approach with the Earth. Despite the short arc of three months, a very large number of optical observations of 2011 MD were collected, precisely 1555. Following the strategy presented in Mommert et al. (2014a), we relaxed the weights for the observations collected during the close approach¹ and we added the Spitzer detection (on 2014 February 11), which extends the observation arc by almost three years.

2015 TC₂₅. Asteroid 2015 TC₂₅ was discovered by the Catalina Sky Survey in October 2015, just two days before an Earth flyby at 0.3 lunar distances. It is one of the smallest asteroids ever discovered, about 2 m in diameter (Reddy et al., 2016), and the 2017 astrometry permits to achieve an estimate of solar radiation pressure. We are aware that for 2015 TC₂₅ the JPL team carried out a specific study (Farnocchia et al., 2017), which adopted *ad hoc*

¹Indeed, timing errors are more relevant for observations performed at small geocentric distances.

weights based on observer-provided uncertainty estimates. To handle this case, we used the same data treatment as JPL.

Note that it is desirable to keep the number of “manual” interventions on the observational data as small as possible. Indeed we are trying to figure out how to automatize the determination of the set of NEAs with significant and reliable Yarkovsky effect. Anyway, in some cases a manual intervention is needed to properly handle observational issues, *e.g.* too much close observations taken during a very close approach and affected by timing errors, remeasurement of old observations.

2.3. Starting sample of NEAs

As first sample of asteroids, we started selecting those objects in NEODyS² having a formal uncertainty on the semimajor axis $\sigma(a) < 3 \cdot 10^{-9}$ au. The choice of the threshold for $\sigma(a)$ comes from an order of magnitude estimate: for an asteroid with diameter 1 km the Yarkovsky drift is about $3 \cdot 10^{-10}$ au/y, thus it causes a variation of $3 \cdot 10^{-9}$ au in ten years. The value of $\sigma(a)$ has to be the one computed at the mean epoch of the observations, since it is the best choice for the orbital fit quality. Moreover, this uncertainty threshold corresponds to a gravity-only fit: after the Yarkovsky coefficient is estimated the uncertainty of the semimajor axis sharply increases because of the strong correlation between A_2 and the semimajor axis.

The list of asteroids satisfying this criterion contained 519 objects (as of February 2018). As a second step, we extracted from the JPL database a set of 89 asteroids having A_2 determined³. Among them, only 16 were not contained in our first list, thus we added them. Furthermore, we considered all the reliable detections from Farnocchia et al. (2013b) and it turned out that only 3 asteroids did not belong to any of the previous lists, thus we added them as well to our sample.

Summarizing, we started with a sample of $519 + 16 + 3 = 538$ objects. For each one of them we performed an orbital fit for the initial conditions together with the Yarkovsky parameter A_2 , without any *a priori* constraint. For few of them we also estimated solar radiation pressure. As a result of the fit, we derived the signal-to-noise ratio SNR_{A_2} of the A_2 parameter, obtaining 101 detections with $\text{SNR}_{A_2} \geq 3$ and 437 with $\text{SNR}_{A_2} < 3$, most of which showing a negligible signal-to-noise ratio.

²The NEODyS database is available at <http://newton.dm.unipi.it>.

³The JPL Small-Body Database is available at <http://ssd.jpl.nasa.gov/sbdb.cgi>.

2.4. Yarkovsky expected value

By means of orbit determination, we determine a transverse acceleration directly from the astrometry. However, to claim that the measured acceleration is caused by the Yarkovsky effect we need to make sure that its magnitude is compatible with the physical properties of the object and the Yarkovsky mechanism. Therefore, we provide an expected value of the Yarkovsky-related orbital drift.

In Farnocchia et al. (2013b), an expected value for A_2 is computed by exploiting the diameter of the asteroid and scaling from the corresponding value of (101955) Bennu, the best determined and reliable Yarkovsky detection. In this paper, we make use of the Yarkovsky calibration as in Spoto et al. (2015):

$$\left(\frac{da}{dt}\right)_{\text{exp}} = \left(\frac{da}{dt}\right)_{\mathcal{B}} \cdot \frac{\sqrt{a_{\mathcal{B}}}(1 - e_{\mathcal{B}}^2)}{\sqrt{a}(1 - e^2)} \frac{D_{\mathcal{B}} \rho_{\mathcal{B}} \cos \phi}{D \rho \cos \phi_{\mathcal{B}}} \frac{1 - A}{1 - A_{\mathcal{B}}}, \quad (2)$$

where D is the diameter of the asteroid, ρ is the density, ϕ is the obliquity (angle between the spin axis and the normal to the orbit plane), and A is the Bond albedo. The latter is computed from the geometric albedo p_v , using $A = \frac{1}{3}p_v$ (Muinonen et al., 2010). The symbols with a “ \mathcal{B} ” refer to asteroid (101955) Bennu, and the values we assume for them are listed in Table 2 with their references.

Table 2: Values of the physical quantities for the asteroid (101955) Bennu, used in equation (2).

Physical quantity	Symbol	Value	Reference
diameter	$D_{\mathcal{B}}$	(0.492 ± 0.020) m	Nolan et al. (2013)
density	$\rho_{\mathcal{B}}$	(1.26 ± 0.07) g/cm ³	Chesley et al. (2014)
geometric albedo	$(p_v)_{\mathcal{B}}$	0.046 ± 0.005	Emery et al. (2014)
obliquity	$\phi_{\mathcal{B}}$	(175 ± 4) deg	Nolan et al. (2013)

For the diameter D we use the known physical value when available. When the asteroid’s shape is not so simple to be approximated by an ellipsoidal model, we use the dynamically equivalent equal volume ellipsoid dimensions to compute the equivalent diameter. In particular, this effort has been done for three asteroids, namely (4179) Toutatis (Hudson et al., 2003), (162421) 2000 ET₇₀ (Naidu et al., 2013), and (275677) 2000 RS₁₁ (Brauer et al., 2015). Otherwise, when no physical information are available, we estimate the diameter from the absolute magnitude H following the relation (Pravec and Harris, 2007)

$$D = 1329 \text{ km} \cdot 10^{-H/5} \cdot \frac{1}{\sqrt{p_v}},$$

where the geometric albedo p_v is assumed to be $p_v = 0.154$ if unknown.

As shown in equation (2), the density is required to estimate the strength of the Yarkovsky effect for asteroids with small diameters. Carry (2012) reports a large number of asteroid densities that we use as starting point. However, in general, density estimates are more reliable and accurate for massive bodies and there is a trend for a decreasing density with diameter, due to the increasing macroporosity⁴ resulting from the cascade of collisions suffered by the body (Carry, 2012; Scheeres et al., 2015). We thus extrapolate the density of small asteroids from the density of large asteroids belonging to the same taxonomic class by increasing their macroporosity to that of Bennu ($\mathcal{P}_B = (40 \pm 10)\%$, from Chesley et al. (2014)). Such macroporosity is typical for (sub-)kilometre-sized asteroids, as illustrated by (25143) Itokawa, visited by the JAXA Hayabusa mission (Fujiwara et al., 2006). This is a modified version of the approach given in Spoto et al. (2015), still using Bennu for the scaling since it has the best estimated Yarkovsky acceleration and a comprehensive physical characterization⁵. Thus the scaled density is given by

$$\rho_s = (1 - \mathcal{P}_B)\rho, \quad (3)$$

where the density scaling factor is $1 - \mathcal{P}_B = 0.60$ and ρ is the known density of the large asteroid. Equation (3) follows from the above assumptions and from the definition of macroporosity. We selected the large asteroids (4) Vesta, (10) Hygiea, (15) Eunomia, and (216) Kleopatra as representative of the taxonomic classes V, C, S, Xe respectively. The density of the representative asteroids and their scaled values are listed in Table 3.

Table 3: Representative asteroids for some taxonomic classes: number/name, taxonomic type, densities as in Carry (2012) with their uncertainties, scaled densities applying the factor $1 - \mathcal{P}_B$.

Asteroid	Tax. type	ρ (g/cm ³)	ρ_s (g/cm ³)
(4) Vesta	V	3.58 ± 0.15	2.15
(10) Hygiea	C	2.19 ± 0.42	1.31
(15) Eunomia	S	3.54 ± 0.20	2.12
(216) Kleopatra	Xe	4.27 ± 0.15	2.56

⁴It is the fraction of volume occupied by voids.

⁵Previously Spoto et al. (2015) used the known density of (704) Interamnia, considered to be a large asteroid with similar composition to Bennu, to estimate porosity of the latter. Recently the composition of (101955) Bennu has been modelled by Clark et al. (2011), based on spectral observations, and it has been found to be closer to other large asteroids, such as (24) Themis and (2) Pallas.

We used three sources of asteroid physical information: the database of physical properties of near-Earth asteroids provided by E.A.R.N.⁶, the JPL Small-Body Database, and the data provided by the WISE mission, such as diameters and albedos (Mainzer et al., 2011). It is important to point out that we have no physical information for the large majority of the objects discussed in this paper. For instance, for the 44% of our detections with $\text{SNR}_{A_2} > 2.5$ we have no physical data, for 62% we have no measured albedo values, and less than half of our detections can be assigned to a taxonomic class.

2.5. Filtering criterion

We use the Yarkovsky-related expected value as a filtering criterion to understand whether the estimated orbital drift da/dt is physically consistent with the Yarkovsky effect. If the estimated da/dt is significantly larger than the maximum absolute expected value (assuming $\cos \phi = \pm 1$), the result is inconsistent with the Yarkovsky mechanism. We compute the indicator parameter

$$\mathcal{S} = \left| \frac{da/dt}{(da/dt)_{\text{exp}}} \right|. \quad (4)$$

Since most times there is very little to no physical information, we need some margin on the upper threshold for \mathcal{S} , which therefore should be larger than 1. We filter out the candidate detections with $\mathcal{S} > 2$. The current maximum value allowed for \mathcal{S} is empirical, but it could be refined. In particular, this upper threshold can be lowered when better data are available. Improving the computation of the expected value - thus decreasing the uncertainty of the indicator parameter \mathcal{S} - requires at least a reliable taxonomic type (for the scaling needed for the density) and better diameters. Values of \mathcal{S} greater than the maximum threshold indicate questionable results. These spurious detections should be investigated to find possible causes and solutions. In general, either the \mathcal{S} value is too high to be compatible with an acceptable detection or it is barely above the maximum threshold, in such a way that additional information would clarify the situation and allow us to decide whether the detection is accepted or refused. For further details see Section 4.

We point out that values $\mathcal{S} \ll 1$ are permitted. Indeed equation (2) employed asteroid size and bulk density, thus $\mathcal{S} \ll 1$ means that the orbital

⁶<http://earn.dlr.de/nea/>

drift is significantly lower than the maximum expected value. Several phenomena can lower the Yarkovsky effect: obliquity $\phi \simeq 90^\circ$, very large or very small thermal inertia, larger density than expected, or small rotation angular velocity. For instance, asteroid (85774) 1998 UT₁₈ has a rotation period of about 34 h, and indeed the indicator \mathcal{S} is low ($\simeq 0.3$, cf. Table 4). The detections of this kind are significant detections of a weak Yarkovsky drift. A second class of weak Yarkovsky drifts can be defined: they are non-detections, that is $\text{SNR}_{A_2} < 3$, but the asteroid has physical properties that would permit a significant detection if the Yarkovsky effect were maximized. Chesley et al. (2016) refer to these detections as weak detections. Despite the low SNR, the result of the A_2 estimation can provide useful constraints on the asteroid’s physical properties.

By combining the value of the SNR_{A_2} coming from the orbital fit with the value of the filtering parameter \mathcal{S} , we divided our detections in three categories.

- We consider *accepted* the detections satisfying both $\text{SNR}_{A_2} \geq 3$ and $\mathcal{S} \leq 2$.
- The category called *marginal significance* includes the asteroids for which $2.5 < \text{SNR}_{A_2} < 3$ and $\mathcal{S} \leq 2$, plus (410777) 2009 FD and (99942) Apophis, both remarkable for their impact monitoring.
- The detections with $\text{SNR}_{A_2} > 3$ and $\mathcal{S} > 2$ are *rejected* because they have a too high value for the indicator parameter \mathcal{S} , suggesting that the detected A_2 signal is unrealistic or not explicable with the Yarkovsky effect (see 2003 RM in Chesley et al. (2016), or (4015) Wilson-Harrington in Section 4).

The results only include detections, that is we do not list the asteroids for which we found no significant Yarkovsky signal from the observational dataset (85% of the initial sample). Figure 1 provides an overall view of our classification. In particular, we consider the plane $(\text{SNR}_{A_2}, \mathcal{S})$ and we mark the detections of each class (but the rejected) with a different color:

- the accepted detections are indicated with a green dot;
- the marginal significance detections are represented with a blue dot, except for (410777) 2009 FD and (99942) Apophis, which are indicated with a blue asterisk (special cases);
- the rejected detections are indicated with a red cross.

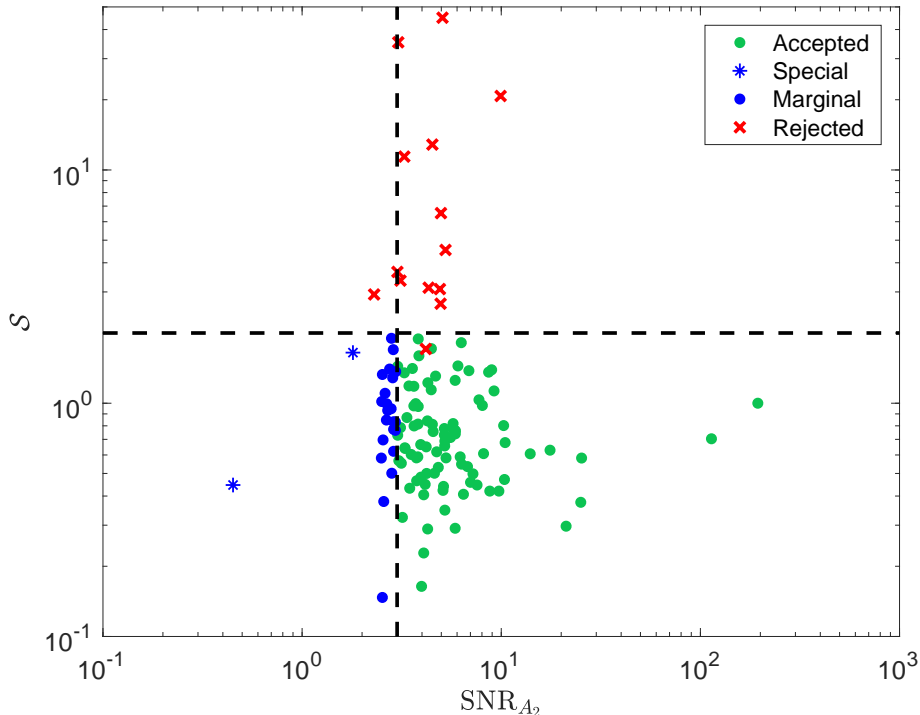


Figure 1: Graphical representation of the partition of the detections set into classes on the plane $(\text{SNR}_{A_2}, \mathcal{S})$. We plot the accepted detections (green dots), the marginally significance detections (blue dots) plus the special cases (410777) 2009 FD and (99942) Apophis (blue asterisk), and the rejected detections (red crosses).

3. Accepted and significant results

As explained in Section 2.3, we started from the initial sample of NEAs and we performed an orbital fit including the Yarkovsky parameter A_2 . Then we applied the filtering procedure, and obtained 87 detections, which are listed in Table 4 and Table 5. For each asteroid, we report the value of the absolute magnitude H , the A_2 parameter along with its uncertainty, the signal-to-noise ratio of A_2 , the value of the semimajor axis drift da/dt , the indicator parameter \mathcal{S} , and the available physical data such as the geometric albedo p_v , the diameter D , the density ρ , and the taxonomic class. As explained in Section 2.4, when no information on the diameter is available, we infer one from the absolute magnitude. We mark these cases with an asterisk (*) in the diameter column. When the albedo is not directly measured but the taxonomic class is known, we assigned the albedo according to Binzel et al. (2002) and marked the albedo value with a dagger (†).

When the albedo is not known we assume $p_v = 0.154$, and mark it with a “d”. Note that 0.154 is a mean value, which has a low probability of being accurate because of the bimodality of the albedo distribution of near-Earth asteroids. Most asteroids are either significantly brighter or significantly darker. Thus, when a diameter D is derived from the absolute magnitude and this default albedo, its relative uncertainty is larger, and in turn the value of \mathcal{S} (containing the factor $1/D$) is uncertain.

Some of the asteroids included in Table 4 and Table 5 deserves dedicated comments.

(1566) *Icarus*.. It is known that the 1968 observations of (1566) Icarus are affected by large timing errors. A possible solution to this problem is to include timing errors in the observations uncertainty possibly even removing the systematic timing errors. A possible alternative is to properly treat the correlation between the right ascension and the declination. This operation will be made easier after the adoption of the new Astrometric Data Exchange Standard (ADES⁷). For now, it is possible to adapt the weighting scheme to underweight the observations during the 1968 close approach: this was done by the JPL team, not by the Pisa one. By comparing the result of the two groups, and also with the one in Greenberg et al. (2017), we can claim that the detection of the Yarkovsky effect is confirmed, even if there is a significant difference between the standard deviations (see Section 7), which is explained by the different weighting scheme.

(3908) *Nyx*.. Asteroid (3908) Nyx is classified as V-type, but it has many properties inconsistent with (4) Vesta. Thus the density scaling is not performed using the density of Vesta as for the other V-type asteroids. Asteroid (5381) Sekhmet is a V-type with a diameter which is comparable to the one of Nyx. The density of Sekhmet is (1.30 ± 0.65) g/cm³ (Carry, 2012), compatible with the estimate in Farnocchia et al. (2014), and we assume this value also for Nyx.

(4179) *Toutatis*. This asteroid shows a significant Yarkovsky detection with $\text{SNR}_{A_2} > 3$ and $\mathcal{S} < 2$ and is therefore included in the list of accepted detections. However, we point out that this detection is subject to substantial uncertainties beyond the formal ones resulting from the fit to the optical and radar astrometry. The large aphelion of the orbit of Toutatis and the

⁷http://minorplanetcenter.net/iau/info/IAU2015_ADES.pdf.

small magnitude of the Yarkovsky perturbation make the A_2 estimate sensitive to the set of main belt perturbers included in the force model and the uncertainty in their masses.

4. Rejected results

In this section we consider the significant detections that we rated as spurious, *i.e.* for which we obtained a Yarkovsky detection greater than one would reasonably expect from the Yarkovsky effect. Despite the signal-to-noise ratio is less than 3, we also add (4015) Wilson-Harrington to this category as a “special” case, as explained below.

Reasons for refusing a detection can be the following:

- Dynamical model problems can occur in few cases, such as (4015) Wilson-Harrington.
- Sometimes the results are strongly dependent on few observations, typically old isolated observations, which are separated by a long time interval from the bulk of the dataset. In these cases we usually reject the detection, unless the precovery has been carefully remeasured, as for (152563) 1992 BF.
- Solutions with Yarkovsky affected by observational data of questionable reliability.

The list of all the rejected detections contains 14 cases, see Table 6. Below we provide dedicated comments for each rejected detection.

(4015) Wilson-Harrington.. This asteroid was initially discovered in 1949 as a comet at the Palomar Sky Survey. It was named 107P/Wilson-Harrington, but then it was lost. Thirty years later the asteroid 1979 VA was discovered and, after the 1988 apparition, it was numbered as (4015) 1979 VA. On August 13, 1992, the IAU circular 5585 (Bowell et al., 1992) reported that the asteroid (4015) 1979 VA and the comet 107P/Wilson-Harrington were indeed the same object. Furthermore, no cometary activity was noted during the well-observed 1979-80 apparition, confirming that it is actually an extinct comet. The detection of the Yarkovsky parameter is indeed significant, but the S value indicates a value of the non-gravitational acceleration that is too large than the one expected from the Yarkovsky effect. Since the observed arc contains the time span of cometary activity, the most likely interpretation is that the large detected transverse acceleration is caused by the out-gassing rather than the Yarkovsky effect. Furthermore, a dynamical

model assuming a constant value for A_2 , as it is the one we employed, is not enough representative of the real orbital dynamics, given that the cometary activity has ceased. Thus in this case we consider that a non-gravitational effect has been detected, but not Yarkovsky.

In some cases, a spurious detections is due to poor optical astrometry, often affecting isolated old observations. In this case we rejected the detection, and a remeasurement of these old observations would be desirable to clarify the situation: the Yarkovsky signal could significantly increase as well as disappear. This is the case for the asteroids listed below.

(260141) 2004 QT₂₄.. The detected signal is strongly dependent on four observations in 1993 and 1998 from Siding Spring Observatory DSS.

(350751) 2002 AW.. This asteroid has two isolated observations in 1991 from Palomar Mountain-DSS.

(39565) 1992 SL.. This asteroid has one isolated observation in 1950 from Palomar Mountain.

(4486) *Mithra*.. This asteroid has a signal which is strongly dependent on a single isolated observation in 1974 from Crimea-Nauchnij (MPC code 095).

(474158) 1999 FA.. This object has one isolated observation in 1978, from Siding Spring Observatory. In agreement with Farnocchia et al. (2013b), we consider that the 1978 observation would need to be remeasured before accepting the Yarkovsky detection for (474158) 1999 FA.

(162421) 2000 ET₇₀.. This asteroid has two isolated observations in 1977 from European Southern Observatory, La Silla DSS.

There are detections which have to be rated as spurious, because \mathcal{S} indicates a Yarkovsky drift which is way larger than expected, despite the fact that the signal-to-noise ratio of the A_2 parameter is greater than 3. This holds for 2010 KP₁₀, (308635) 2005 YU₅₅, (139359) 2001 ME₁, (142561) 2002 TX₆₈, and (192563) 1998 WZ₆. To confirm the reliability of our filtering criterion, we carefully checked each of these spurious detections. They show problematic astrometry, which resulted in a incorrect determination of the Yarkovsky effect.

A separate comment holds for (175706) 1996 FG₃, since it is a binary asteroid (Scheirich et al., 2015). The signal found for the Yarkovsky detection is likely due to the astrometric data treatment, as confirmed by the

fact that it disappears when the weighting scheme proposed in Vereš et al. (2017) is applied. Once we have a Yarkovsky detection for this object it will be possible to compare with the Yarkovsky theory for binary asteroids as described by Vokrouhlický et al. (2005).

A remarkable case is (433) Eros. This asteroid shows a significant value for the Yarkovsky effect, but a very high value for the indicator parameter. Moreover, the obliquity of Eros is known to be $\simeq 89^\circ$ (Yeomans et al., 2000), therefore we would expect a value for \mathcal{S} much less than 1. Thus this detection is spurious, likely caused by historical data dating back to 1893 for which it is challenging to come up with a reliable statistical treatment.

5. Marginal significance

We now consider the marginal significance class, containing the detections for which $2.5 < \text{SNR}_{A_2} < 3$ and $\mathcal{S} \leq 2$. These detections are physically meaningful since they satisfy the filtering on \mathcal{S} , but the signal to noise for the A_2 parameter as determined from the observations is not enough for a reliable detection. In addition, as mentioned before, we include two special cases in this category, namely (410777) 2009 FD and (99942) Apophis. These two objects show acceptable values of the indicator \mathcal{S} but the signal-to-noise ratio of the A_2 parameter is very low (cf. Table 7). Nevertheless, we decided to keep them because the Yarkovsky drift plays a fundamental role for its impact predictions (see the introduction). In this way we grouped 24 detections in this class, which are listed in Table 7.

(99942) Apophis.. Similarly to Toutatis, also Apophis has a complex rotation, as shown in Pravec et al. (2014); Vokrouhlický et al. (2015b). However, the Yarkovsky effect is not significantly weakened by the tumbling state. Vokrouhlický et al. (2015b) used the available rotation state, shape, size and thermophysical model of Apophis to predict the Yarkovsky semimajor axis drift. The drift obtained by fitting the astrometric data is compatible with the model prediction. We obtained $da/dt = (-24.50 \pm 13.58) \cdot 10^{-4}$ au/Myr for the fitted value, which is completely consistent with Vokrouhlický et al. (2015b). There is no question that the Yarkovsky effect has to be taken into account for Apophis to predict future motion, especially for impact hazard assessment (Chesley, 2006; Giorgini et al., 2008; Farnocchia et al., 2013a).

(410777) 2009 FD.. The Yarkovsky effect found is below the significance level, and nevertheless it has to be taken into account for long-term impact monitoring purposes (Spoto et al., 2014).

Maintaining a list of marginal significance detections is useful because they are candidates for future detections as observational data improves and increases.

6. Direct radiation pressure detection

Solar radiation pressure is a more complicated perturbation to detect. So far, solar radiation pressure has only been detected for very small objects ($H > 27$) who experienced Earth encounters. Thus we started selecting the smallest asteroids of the initial sample (more precisely, those with $H > 24$) since the effect becomes larger for smaller size objects, and we tried to detect solar radiation pressure (SRP) along with the Yarkovsky parameter.

The acceleration caused by solar radiation pressure is radial and can be modelled with a single parameter A_1 ,

$$\mathbf{a}_r = A_1 g(r) \hat{\mathbf{r}}.$$

In this equation A_1 is a free parameter, and $g(r) = 1/r^2$, where r is the heliocentric distance in astronomical units. Physically, the value of A_1 depends mostly on the the area-to-mass ratio \mathcal{A}/M . The relation between them is the following

$$A_1 = \frac{\Phi_{\odot}}{c} \cdot C_R \cdot \mathcal{A}/M,$$

where c is the speed of light, Φ_{\odot} is the solar radiation energy flux at 1 au, whose value is $\Phi_{\odot} \simeq 1.361 \text{ kW/m}^2$, and C_R is a coefficient (of the order of 1) depending upon shape and optical properties of the surface.

The starting sample of asteroids for which we attempted an 8-dimensional fit contained 10 objects. We found four accepted detections, *i.e.* $\text{SNR}_{A_1} \geq 3$, which are listed in Table 8. Notice that for three asteroids of this category, namely 2011 MD, 2012 LA, and 2015 TC₂₅, the Yarkovsky detection is not significant and thus the \mathcal{S} value, though above the threshold in one case, does not provide any information. Concerning the area-to-mass ratio we would compare the value of \mathcal{A}/M with an expected value, as we do with the secular semimajor axis drift da/dt , but this is not possible for now since the diameter is very uncertain and the other physical properties are currently unknown. Other fitted values of the area-to-mass ratio has already been determined for 2009 BD (Micheli et al., 2012), 2012 LA (Micheli et al., 2013) and 2011 MD (Micheli et al., 2014), though without including the Yarkovsky effect in the dynamical model. Asteroid 2006 RH₁₂₀ is listed separately from the others, since we consider it spurious, as we explain in what follows.

2006 RH₁₂₀.. This strange detection has already been discussed in Chesley et al. (2016). Our results are very compatible with those of that paper, and we agree with the motivations provided to reject this detection. The most likely explanation for the high transverse acceleration can be the presence of some non-conservative force, *e.g.* mass-shedding, outgassing or micrometeorite flux, that can become as relevant as the Yarkovsky effect for objects of this size. The area-to-mass ratio, which results in a significant detection, is not compatible with the hypothesis that 2006 RH₁₂₀ is an artificial object.

7. Comparison with JPL results

As we already mentioned, the JPL database is regularly updated with the asteroids for which the orbital fit shows evidence of the Yarkovsky effect. The same is done for solar radiation pressure when appropriate. The results produced by two independent software are expected to be different, but compatible. In order to compare them we compute the relative errors

$$\varepsilon_r(A_2) := \frac{|A_2 - A_2^{\text{JPL}}|}{\sigma_{A_2}} \quad \text{and} \quad \varepsilon_r^{\text{JPL}}(A_2) := \frac{|A_2 - A_2^{\text{JPL}}|}{\sigma_{A_2, \text{JPL}}},$$

where the superscript “JPL” refers to the JPL solution. To quantify the difference between the results presented in this paper and the JPL ones, we use the quantity

$$\chi_{A_2} := \frac{|A_2 - A_2^{\text{JPL}}|}{\sqrt{\sigma_{A_2}^2 + \sigma_{A_2, \text{JPL}}^2}}$$

from (Milani and Gronchi, 2010, Sec. 7.2). We consider compatible two solutions for which $\chi_{A_2} \leq 1$.

Starting from the list of our accepted detections, we compared the results every time an asteroid is included in the JPL database of Yarkovsky effect detections. The results of the comparison are contained in Table 9 and 10. Just for five asteroids in this list both the relative errors are greater than 1, even though never above 2.5. Using the metric given by χ_{A_2} , we identify just 3 asteroids (marked with a star in Table 9 and 10) whose detections are not fully compatible with respect to our criteria. Anyway, a χ_{A_2} moderately above 1 for 3 cases out of 92 being compared shows a strong agreement between our results and the JPL’s ones.

Note that this result is not a null test, that is the expected value of the difference in the estimated values of A_2 is not zero. This because the two computations have used two different astrometric error models, Farnocchia et al. (2015a) at NEODyS and Vereš et al. (2017) at JPL. The

comparative results described in the last three columns indicate an exceptionally good agreement. This agreement may be interpreted as a validation of the procedures used both at NEODyS and at JPL, both to compute the Yarkovsky effect constants and to select the cases in which the results are reliable.

The comparison was also performed for the shorter list of objects for which we have both A_2 and A_1 , that is both Yarkovsky effect and direct radiation pressure were included in the dynamical model. Table 11 contains the signal-to-noise ratios for both parameters in both solutions, and all the metrics for the discrepancies. Apart from the results for 2006 RH₁₂₀, which are rated as spurious, the accepted results are fully consistent.

8. Impact monitoring with non-gravitational parameters

A force model including non-gravitational forces is sometimes needed to make reliable impact predictions, especially if we want to extend the hazard analysis time span to longer intervals with respect to one century (the default time span adopted by the current impact monitoring systems). More precisely, the non-gravitational model plays a fundamental role also in the Line Of Variations (LOV) computation and propagation (Milani et al., 2005; Milani et al., 2005, 2000). If an asteroid with a very well constrained orbit experiences a very deep close approach, the post-encounter situation is equal to the one of a poorly determined orbit, with the difference that the large uncertainty of the asteroid state is due to the divergence of nearby orbits caused by the encounter, and not to the poor constraints of the initial conditions. In this case, the initial confidence region is very small, thus the use of the linear approximation of the LOV is allowed. In case such an encounter occurs the linear LOV direction is derived by analyzing that encounter and mapping back the corresponding LOV trace on the target plane (TP) (Valsecchi et al., 2003) to the space of initial conditions. This method has been used in Spoto et al. (2014) to properly assess the impact risk of (410777) 2009 FD, exploiting its 2185 scattering encounter with the Earth. The same formalism can be used even when we are not in the presence of a scattering encounter, but the close encounter is so deep that the LOV will turn out to be quite stretched at the next encounter, as in the cases analyzed below.

So far, just four asteroids required such special treatment for a proper impact risk assessment, namely (101955) Bennu, (99942) Apophis, (29075) 1950 DA, and (410777) 2009 FD, but this list is expected to grow as a consequence of the work presented in this paper. Below we show two examples

of asteroids for which we found virtual impactors using a non-gravitational model and that have no possible impacts with a purely gravitational model. We are aware that such a work could be done on many asteroids with accepted Yarkovsky detections, but this is beyond the scope of this paper.

2001 BB₁₆.. Currently, this asteroid has a low MOID value, $\simeq 0.0043$ au, but no chance of impacting the Earth in the next century. 2001 BB₁₆ has a deep close approach with the Earth in 2082, which causes an increase of the stretching of two orders of magnitude with respect to the next 2086 encounter, whereas the stretching value remains essentially constant until the 2082 close approach. We used this close approach to derive the LOV direction and we performed the impact monitoring through 2200 employing a non-gravitational model including the Yarkovsky effect. The results are shown in Table 12. In particular we found two VIs at the very end of the 22nd century, which we would not find with a gravity-only model.

2011 MD.. This is a very small asteroid, about 6 m in diameter, as determined in Mommert et al. (2014a). In this case as well, the MOID value is very low, $\simeq 0.00036$ au and it has no virtual impactor in the next century. In 2049, this asteroid will experience two very close approaches with the Earth, causing an increase of two orders of magnitude in the stretching between these encounters and the following one in 2067. We used the first 2049 close approach (the deepest of the two) to compute the LOV direction in the space of initial conditions. We thus performed the impact monitoring using a dynamical model including both the Yarkovsky effect and solar radiation pressure. The results are shown in Table 13. When we only include solar radiation pressure, the orbit uncertainty shrinks and thus the number of VIs is much lower than before (see Table 14). Both Table 13 and Table 14 list the virtual impactors with $IP \geq 10^{-7}$, since this threshold is the completeness limit used for the LOV sampling (Del Vigna et al., 2018).

It is worth noting that this asteroid is so small that it would not reach the Earth in case of a real impact, because it would be burnt in the atmosphere. This case is studied to show that, in some cases, a non-gravitational model is needed to make reliable impact predictions and also that different models of non-gravitational perturbations can give very different results.

9. Conclusions and future work

In this paper we significantly increased the knowledge of non-gravitational perturbations on near-Earth asteroids, based on actual measurements, rather

than on modelling. The number of significant and reliable Yarkovsky detections in the NEA catalog is expected to grow continuously. In fact, the data volume of future surveys, the increased astrometric accuracy for optical observations, more accurate star catalog debiasing techniques, and expanded efforts in radar astrometry provide ever better constraints to measure this small effect. We identified 87 near-Earth asteroids with significant and reliable Yarkovsky detection, thus doubling the list provided in Chesley et al. (2016). For few exceedingly small asteroids, we attempted to directly detect solar radiation pressure together with the Yarkovsky-related acceleration. For such cases, solar radiation pressure is needed to obtain a more satisfactory orbital fit.

There are several research centers handling the computation of asteroid orbits as an industrial production, like recomputing either all the orbits of more than 500,000 numbered asteroids every time a change in the error model occurs, or a large portion of them just to take into account new observations and new asteroid discoveries⁸. There are important scientific goals such as asteroid families and impact monitoring that can only be achieved by maintaining and constantly updating such large lists of orbits.

We dedicated a significant effort in clarifying a number of marginal and/or spurious cases, not only to recover few dubious cases but also to refine the methodology and therefore be ready for the future increase of significant detections. Indeed, the problem to be faced in the near future is not another increase by a factor two, rather an increase by orders of magnitude. The second Gaia data release (April 2018) will contain about 1.7 billion of sources brighter than magnitude 21 and $\simeq 14000$ asteroids with astrometry reaching the sub-milliarcsec accuracy in an optimal range of magnitude $G \simeq 12 - 17$ (Gaia Collaboration et al., 2018a,b). The stellar catalog produced by Gaia will represent the starting point for a new debiasing and weighting scheme. Moreover, the combination of Gaia asteroid observations with the already available ones will produce a sharp increase in the number of objects for which the Yarkovsky effect will be detectable. Thus the challenge in papers like this is not to establish a new record list of Yarkovsky and/or radiation pressure detections, but rather to develop an automated calculation of orbits with estimated non-gravitational parameters.

The computations of orbits with non-gravitational effects is still very far from being an automated process. To avoid spurious detections, we used the

⁸The authors of this paper all belong to four centers performing this kind of activity: NEODyS, JPL, IMCCE, NEOCC.

most recent error models for the observations and a filtering criterion, based on an estimate of the Yarkovsky effect based upon a physical model of the asteroid. Unfortunately, both of these tools are still incomplete. The error models suffer from the continued unavailability of metadata, such as the signal-to-noise of individual observations, with the result that observations with different quality are bundled together and the statistical analysis of the residuals does not yet allow a correct derivation of uncertainty of the measurement error. The physical models of asteroids, needed to estimate the expected Yarkovsky effect, are very rough approximations when the main physical data are not available, as it is the case for the majority of the asteroids in our tables. Moreover, such small perturbations can be sensitive to old isolated, and possibly bad astrometric positions.

In conclusion, we made a step in the right direction by developing and testing the use of different error models, and by using the difference in the results as an estimate of the sensitivity of the results on the error model. We developed and tested the use of a filter for spurious cases, which is based on an estimate of the expected Yarkovsky effect, which is roughly the same as the Yarkovsky calibration used to compute the age of asteroid families Milani et al. (2014); Spoto et al. (2015). Both tools improved our capability of obtaining a list of reliable Yarkovsky detections, as well as a much shorter list of radiation pressure detections for natural bodies.

Acknowledgements

We thank the referee Dr. David Vokrouhlicky for his useful comments that have improved the quality of the paper.

A. Del Vigna and L. Faggioli acknowledges support by the company SpaceDyS. D. Farnocchia conducted this research at the Jet Propulsion Laboratory, California Institute of Technology, under a contract with NASA.

This research was conducted under European Space Agency contract No. 4000113555/15/DMRP “P2-NEO-II Improved NEO Data Processing Capabilities”.

References

- Baer, J., Chesley, S. R., Matson, R. D., May 2011. Astrometric Masses of 26 Asteroids and Observations on Asteroid Porosity. *AJ*141, 143.
- Binzel, R. P., Lupishko, D., di Martino, M., Whiteley, R. J., Hahn, G. J., Mar. 2002. Physical Properties of Near-Earth Objects. University of Arizona Press.

- Bowell, E., West, R. M., Heyer, H.-H., Quebatte, J., Cunningham, L. E., Bus, S. J., Harris, A. W., Millis, R. L., Marsden, B. G., Aug. 1992. (4015) 1979 VA = Comet Wilson-Harrington (1949 III). IAU Circ.5585.
- Brauer, K., Busch, M. W., Benner, L. A. M., Brozovic, M., Howell, E. S., Nolan, M. C., Springmann, A., Giorgini, J. D., Taylor, P. A., Jao, J. S., Nov. 2015. The Shape of Near-Earth Asteroid 275677 (2000 RS11) From Inversion of Arecibo and Goldstone Radar Images. In: AAS/Division for Planetary Sciences Meeting Abstracts. Vol. 47 of AAS/Division for Planetary Sciences Meeting Abstracts.
- Carpino, M., Milani, A., Chesley, S. R., Dec. 2003. Error statistics of asteroid optical astrometric observations. *Icarus*166, 248–270.
- Carry, B., Dec. 2012. Density of asteroids. *Planet. Space Sci.*73, 98–118.
- Chesley, S. R., 2006. Potential impact detection for Near-Earth asteroids: the case of 99942 Apophis (2004 MN4). In: Daniela, L., Sylvio Ferraz, M., Angel, F. J. (Eds.), *Asteroids, Comets, Meteors*. Vol. 229 of IAU Symposium. pp. 215–228.
- Chesley, S. R., Farnocchia, D., Nolan, M. C., Vokrouhlický, D., Chodas, P. W., Milani, A., Spoto, F., Rozitis, B., Benner, L. A. M., Bottke, W. F., Busch, M. W., Emery, J. P., Howell, E. S., Lauretta, D. S., Margot, J.-L., Taylor, P. A., Jun. 2014. Orbit and bulk density of the OSIRIS-REx target Asteroid (101955) Bennu. *Icarus* 235, 5–22.
- Chesley, S. R., Farnocchia, D., Pravec, P., Vokrouhlický, D., Jan. 2016. Direct Detections of the Yarkovsky Effect: Status and Outlook. In: Chesley, S. R., Morbidelli, A., Jedicke, R., Farnocchia, D. (Eds.), *Asteroids: New Observations, New Models*. Vol. 318 of IAU Symposium. pp. 250–258.
- Chesley, S. R., Ostro, S. J., Vokrouhlický, D., Čapek, D., Giorgini, J. D., Nolan, M. C., Margot, J.-L., Hine, A. A., Benner, L. A. M., Chamberlin, A. B., Dec. 2003. Direct Detection of the Yarkovsky Effect by Radar Ranging to Asteroid 6489 Golevka. *Science* 302, 1739–1742.
- Clark, B. E., Binzel, R. P., Howell, E. S., Cloutis, E. A., Ockert-Bell, M., Christensen, P., Barucci, M. A., DeMeo, F., Lauretta, D. S., Connolly, H., Soderberg, A., Hergenrother, C., Lim, L., Emery, J., Mueller, M., Dec. 2011. Asteroid (101955) 1999 RQ36: Spectroscopy from 0.4 to 2.4 μm and meteorite analogs. *Icarus*216, 462–475.

- Del Vigna, A., Milani, A., Spoto, F., Chessa, A., Valsecchi, G. B., 2018. Completeness of Impact Monitoring. *Icarus*. *Submitted*.
- Einstein, A., Infeld, L., Hoffmann, B., 1938. The gravitational equations and the problem of motion. *Annals of Mathematics* 39 (1), 65–100.
- Emery, J. P., Fernández, Y. R., Kelley, M. S. P., Warden (née Crane), K. T., Hergenrother, C., Lauretta, D. S., Drake, M. J., Campins, H., Ziffer, J., May 2014. Thermal infrared observations and thermophysical characterization of OSIRIS-REx target asteroid (101955) Bennu. *Icarus*234, 17–35.
- Farnocchia, D., Chesley, S. R., Feb. 2014. Assessment of the 2880 impact threat from Asteroid (29075) 1950 DA. *Icarus*229, 321–327.
- Farnocchia, D., Chesley, S. R., Chamberlin, A. B., Tholen, D. J., Jan. 2015a. Star catalog position and proper motion corrections in asteroid astrometry. *Icarus*245, 94–111.
- Farnocchia, D., Chesley, S. R., Chodas, P. W., Micheli, M., Tholen, D. J., Milani, A., Elliott, G. T., Bernardi, F., May 2013a. Yarkovsky-driven impact risk analysis for asteroid (99942) Apophis. *Icarus* 224, 192–200.
- Farnocchia, D., Chesley, S. R., Milani, A., Gronchi, G. F., Chodas, P. W., 2015b. Orbits, Long-Term Predictions, Impact Monitoring. In: Michel, P., DeMeo, F. E., Bottke, W. F. (Eds.), *Asteroids IV*. University of Arizona Press, pp. 815–834.
- Farnocchia, D., Chesley, S. R., Tholen, D. J., Micheli, M., Aug. 2014. High precision predictions for near-Earth asteroids: the strange case of (3908) Nyx. *Celestial Mechanics and Dynamical Astronomy* 119 (3), 301–312.
- Farnocchia, D., Chesley, S. R., Vokrouhlický, D., Milani, A., Spoto, F., Bottke, W. F., May 2013b. Near Earth Asteroids with measurable Yarkovsky effect. *Icarus* 224, 1–13.
- Farnocchia, D., Tholen, D. J., Micheli, M., Ryan, W., Rivera-Valentin, E. G., Taylor, P. A., Giorgini, J. D., Oct. 2017. Mass estimate and close approaches of near-Earth asteroid 2015 TC25. In: *AAS/Division for Planetary Sciences Meeting Abstracts #49*. Vol. 49 of *AAS/Division for Planetary Sciences Meeting Abstracts*. p. 100.09.
- Folkner, W. M., Williams, J. G., Boggs, D. H., Park, R. S., Kuchynka, P., Feb. 2014. The Planetary and Lunar Ephemerides DE430 and DE431. *Interplanetary Network Progress Report* 196, 1–81.

- Fujiwara, A., Kawaguchi, J., Yeomans, D. K., Abe, M., Mukai, T., Okada, T., Saito, J., Yano, H., Yoshikawa, M., Scheeres, D. J., Barnouin-Jha, O., Cheng, A. F., Demura, H., Gaskell, R. W., Hirata, N., Ikeda, H., Kominato, T., Miyamoto, H., Nakamura, A. M., Nakamura, R., Sasaki, S., Uesugi, K., Jun. 2006. The Rubble-Pile Asteroid Itokawa as Observed by Hayabusa. *Science* 312, 1330–1334.
- Gaia Collaboration, Brown, A. G. A., Vallenari, A., Prusti, T., de Bruijne, J. H. J., Babusiaux, C., Bailer-Jones, C. A. L., 2018a. Gaia data release 2 summary of the contents and survey properties. *Astronomy & Astrophysics*.
- Gaia Collaboration, Spoto, F., Tanga, P., Mignard, F., Berthier, J., Carry, B., Cellino, A., 2018b. Gaia data release 2: observations of solar system objects. *Astronomy & Astrophysics*.
- Giorgini, J. D., Benner, L. A. M., Ostro, S. J., Nolan, M. C., Busch, M. W., Jan. 2008. Predicting the Earth encounters of (99942) Apophis. *Icarus* 193, 1–19.
- Giorgini, J. D., Ostro, S. J., Benner, L. A. M., Chodas, P. W., Chesley, S. R., Hudson, R. S., Nolan, M. C., Klemola, A. R., Standish, E. M., Jurgens, R. F., Rose, R., Chamberlin, A. B., Yeomans, D. K., Margot, J.-L., Sep. 2002. Asteroid 1950 DA’s Encounter with Earth in 2880: Physical Limits of Collision Probability Prediction. In: AAS/Division of Dynamical Astronomy Meeting #33. Vol. 34 of *Bulletin of the American Astronomical Society*. p. 934.
- Greenberg, A. H., Margot, J.-L., Verma, A. K., Taylor, P. A., Naidu, S. P., Brozovic, M., Benner, L. A. M., Mar. 2017. Asteroid 1566 Icarus’s Size, Shape, Orbit, and Yarkovsky Drift from Radar Observations. *AJ* 153, 108.
- Hudson, R. S., Ostro, S. J., Scheeres, D. J., Feb. 2003. High-resolution model of Asteroid 4179 Toutatis. *Icarus* 161, 346–355.
- Konopliv, A. S., Asmar, S. W., Folkner, W. M., Karatekin, Ö., Nunes, D. C., Smrekar, S. E., Yoder, C. F., Zuber, M. T., Jan. 2011. Mars high resolution gravity fields from MRO, Mars seasonal gravity, and other dynamical parameters. *Icarus* 211, 401–428.
- Mainzer, A., Grav, T., Bauer, J., Masiero, J., McMillan, R. S., Cutri, R. M., Walker, R., Wright, E., Eisenhardt, P., Tholen, D. J., Spahr, T., Jedicke, R., Denneau, L., DeBaun, E., Elsbury, D., Gautier, T., Gomillion, S.,

- Hand, E., Mo, W., Watkins, J., Wilkins, A., Bryngelson, G. L., Del Pino Molina, A., Desai, S., Gómez Camus, M., Hidalgo, S. L., Konstantopoulos, I., Larsen, J. A., Maleszewski, C., Malkan, M. A., Mauduit, J.-C., Mullan, B. L., Olszewski, E. W., Pforr, J., Saro, A., Scotti, J. V., Wasserman, L. H., Dec. 2011. NEOWISE Observations of Near-Earth Objects: Preliminary Results. *ApJ*743, 156.
- Marsden, B. G., Sekanina, Z., Yeomans, D. K., Mar. 1973. Comets and nongravitational forces. V. *Astronomical Journal* 78, 211.
- Micheli, M., Tholen, D. J., Elliott, G. T., May 2012. Detection of radiation pressure acting on 2009 BD. *New A*17, 446–452.
- Micheli, M., Tholen, D. J., Elliott, G. T., Sep. 2013. 2012 LA, an optimal astrometric target for radiation pressure detection. *Icarus*226, 251–255.
- Micheli, M., Tholen, D. J., Elliott, G. T., Jun. 2014. Radiation Pressure Detection and Density Estimate for 2011 MD. *ApJ*788, L1.
- Milani, A., Cellino, A., Knežević, Z., Novaković, B., Spoto, F., Paolicchi, P., Sep. 2014. Asteroid families classification: Exploiting very large datasets. *Icarus* 239, 46–73.
- Milani, A., Chesley, S. R., Sansaturio, M. E., Bernardi, F., Valsecchi, G. B., Arratia, O., Oct. 2009. Long term impact risk for (101955) 1999_{RQ}36. *Icarus* 203, 460–471.
- Milani, A., Chesley, S. R., Sansaturio, M. E., Tommei, G., Valsecchi, G. B., Feb. 2005. Nonlinear impact monitoring: line of variation searches for impactors. *Icarus* 173, 362–384.
- Milani, A., Chesley, S. R., Valsecchi, G. B., Aug. 2000. Asteroid close encounters with Earth: risk assessment. *Planet. Space Sci.*48, 945–954.
- Milani, A., Gronchi, G. F., 2010. *Theory of Orbit Determination*. Cambridge University Press.
- Milani, A., Sansaturio, M., Tommei, G., Arratia, O., Chesley, S. R., Feb. 2005. Multiple solutions for asteroid orbits: Computational procedure and applications. *Astronomy & Astrophysics* 431, 729–746.
- Mommert, M., Farnocchia, D., Hora, J. L., Chesley, S. R., Trilling, D. E., Chodas, P. W., Mueller, M., Harris, A. W., Smith, H. A., Fazio, G. G., Jul. 2014a. Physical Properties of Near-Earth Asteroid 2011 MD. *ApJ*789, L22.

- Mommert, M., Hora, J. L., Farnocchia, D., Chesley, S. R., Vokrouhlický, D., Trilling, D. E., Mueller, M., Harris, A. W., Smith, H. A., Fazio, G. G., May 2014b. Constraining the Physical Properties of Near-Earth Object 2009 BD. *ApJ*786, 148.
- Moyer, T., 2003. Formulation for observed and computed values of Deep Space Network data types for navigation. Deep-space communications and navigation series. Wiley-Interscience.
- Muinsonen, K., Belskaya, I. N., Cellino, A., Delbò, M., Lévassieur-Regourd, A.-C., Penttilä, A., Tedesco, E. F., Oct. 2010. A three-parameter magnitude phase function for asteroids. *Icarus*209, 542–555.
- Naidu, S. P., Margot, J.-L., Busch, M. W., Taylor, P. A., Nolan, M. C., Brozovic, M., Benner, L. A. M., Giorgini, J. D., Magri, C., Sep. 2013. Radar imaging and physical characterization of near-Earth Asteroid (162421) 2000 ET70. *Icarus*226, 323–335.
- Nolan, M. C., Magri, C., Howell, E. S., Benner, L. A. M., Giorgini, J. D., Hergenrother, C. W., Hudson, R. S., Lauretta, D. S., Margot, J.-L., Ostro, S. J., Scheeres, D. J., Sep. 2013. Shape model and surface properties of the OSIRIS-REx target Asteroid (101955) Bennu from radar and lightcurve observations. *Icarus*226, 629–640.
- Nugent, C. R., Margot, J. L., Chesley, S. R., Vokrouhlický, D., Aug. 2012. Detection of Semimajor Axis Drifts in 54 Near-Earth Asteroids: New Measurements of the Yarkovsky Effect. *AJ*144, 60.
- Pravec, P., Harris, A. W., Sep. 2007. Binary asteroid population. 1. Angular momentum content. *Icarus*190, 250–259.
- Pravec, P., Scheirich, P., Ďurech, J., Pollock, J., Kušnirák, P., Hornoch, K., Galád, A., Vokrouhlický, D., Harris, A. W., Jehin, E., Manfroid, J., Opitom, C., Gillon, M., Colas, F., Oey, J., Vraštil, J., Reichart, D., Ivarsen, K., Haislip, J., LaCluyze, A., May 2014. The tumbling spin state of (99942) Apophis. *Icarus*233, 48–60.
- Reddy, V., Sanchez, J. A., Bottke, W. F., Thirouin, A., Rivera-Valentin, E. G., Kelley, M. S., Ryan, W., Cloutis, E. A., Tegler, S. C., Ryan, E. V., Taylor, P. A., Richardson, J. E., Moskovitz, N., Le Corre, L., Dec. 2016. Physical Characterization of ~ 2 -meter Diameter Near-Earth Asteroid 2015 TC₂₅: A Possible Boulder from E-type Asteroid (44) Nysa. *AJ*152, 162.

- Rozitis, B., Maclennan, E., Emery, J. P., Aug. 2014. Cohesive forces prevent the rotational breakup of rubble-pile asteroid (29075) 1950 DA. *Nature* 512, 174–176.
- Scheeres, D. J., Britt, D., Carry, B., Holsapple, K. A., 2015. Asteroid Interiors and Morphology. pp. 745–766.
- Scheirich, P., Pravec, P., Jacobson, S. A., Ďurech, J., Kušnirák, P., Hornoch, K., Mottola, S., Mommert, M., Hellmich, S., Pray, D., Polishook, D., Krugly, Y. N., Inasaridze, R. Y., Kvaratskhelia, O. I., Ayvazian, V., Slyusarev, I., Pittichová, J., Jehin, E., Manfroid, J., Gillon, M., Galád, A., Pollock, J., Licandro, J., Alí-Lagoa, V., Brinsfield, J., Molotov, I. E., Jan. 2015. The binary near-Earth Asteroid (175706) 1996 FG₃ - An observational constraint on its orbital evolution. *Icarus* 245, 56–63.
- Spoto, F., Milani, A., Farnocchia, D., Chesley, S. R., Micheli, M., Valsecchi, G. B., Perna, D., Hainaut, O., Dec. 2014. Nongravitational perturbations and virtual impactors: the case of asteroid (410777) 2009 FD. *Astronomy & Astrophysics* 572.
- Spoto, F., Milani, A., Knežević, Z., Sep. 2015. Asteroid family ages. *Icarus* 257, 275–289.
- Standish, E. M., Hellings, R. W., Aug. 1989. A determination of the masses of Ceres, Pallas, and Vesta from their perturbations upon the orbit of Mars. *Icarus* 80, 326–333.
- Tardioli, C., Farnocchia, D., Rozitis, B., Cotto-Figueroa, D., Chesley, S. R., Statler, T. S., Vasile, M., Dec. 2017. Constraints on the near-Earth asteroid obliquity distribution from the Yarkovsky effect. *A&A* 608, A61.
- Valsecchi, G. B., Milani, A., Gronchi, G. F., Chesley, S. R., 2003. Resonant returns to close approaches: Analytical theory. *Astronomy & Astrophysics* 408, 1179–1196.
- Vereš, P., Farnocchia, D., Chesley, S. R., Chamberlin, A. B., Nov. 2017. Statistical analysis of astrometric errors for the most productive asteroid surveys. *Icarus* 296, 139–149.
- Vokrouhlický, D., Bottke, W. F., Chesley, S. R., Scheeres, D. J., Statler, T. S., 2015a. The Yarkovsky and YORP Effects. In: Michel, P., DeMeo, F. E., Bottke, W. F. (Eds.), *Asteroids IV*. University of Arizona Press, pp. 509–531.

- Vokrouhlický, D., Brož, M., Bottke, W. F., Nesvorný, D., Morbidelli, A., May 2006. Yarkovsky/YORP chronology of asteroid families. *Icarus*182, 118–142.
- Vokrouhlický, D., Chesley, S. R., Matson, R. D., Jun. 2008. Orbital Identification for Asteroid 152563 (1992 BF) Through the Yarkovsky Effect. *Astronomical Journal* 135, 2336–2340.
- Vokrouhlický, D., Farnocchia, D., Čapek, D., Chesley, S. R., Pravec, P., Scheirich, P., Müller, T. G., May 2015b. The Yarkovsky effect for 99942 Apophis. *Icarus*252, 277–283.
- Vokrouhlický, D., Milani, A., Chesley, S. R., Nov. 2000. Yarkovsky Effect on Small Near-Earth Asteroids: Mathematical Formulation and Examples. *Icarus* 148, 118–138.
- Vokrouhlický, D., Čapek, D., Chesley, S. R., Ostro, S. J., Dec. 2005. Yarkovsky detection opportunities. II. Binary systems. *Icarus*179, 128–138.
- Will, C. M., Mar. 1993. *Theory and Experiment in Gravitational Physics*. Cambridge University Press.
- Yeomans, D. K., Antreasian, P. G., Barriot, J.-P., Chesley, S. R., Dunham, D. W., Farquhar, R. W., Giorgini, J. D., Helfrich, C. E., Konopliv, A. S., McAdams, J. V., Miller, J. K., Owen, W. M., Scheeres, D. J., Thomas, P. C., Veverka, J., Williams, B. G., Sep. 2000. Radio Science Results During the NEAR-Shoemaker Spacecraft Rendezvous with Eros. *Science* 289, 2085–2088.

Table 4: List of Yarkovsky detections with $\text{SNR}_{A_2} > 5$ and with $\mathcal{S} \leq 2$. The table is sorted by SNR_{A_2} , in decreasing order. The columns contain the asteroid name, the absolute magnitude H , the A_2 parameter with its uncertainty and signal-to-noise ratio SNR_{A_2} , the semimajor axis drift da/dt with its uncertainty, the indicator parameter \mathcal{S} , the geometric albedo p_v , the diameter D and the taxonomic class. Asteroids with no available information about the diameter are marked with an asterisk (*). Asteroids with albedo assigned according to Binzel et al. (2002) since no direct estimate is available are marked with a “d”. Asteroids with no albedo informations are marked with a dagger (†). A remarkable detection is that of asteroid (480883) 2001 YE₄. This detection was not in the list of valid detections provided in Chesley et al. (2016), whereas in the present work it has a very high SNR_{A_2} value. The substantial difference lies in the radar observations of December 2016, confirming that radar is a very powerful tool in getting specifically high signal-to-noise ratio Yarkovsky detections.

Asteroid	H	A_2 (10^{-15} au/d ²)	SNR_{A_2}	da/dt (10^{-4} au/My)	\mathcal{S}	p_v	D (km)	Tax. class
(101955) Bennu	20.6	-46.20 ± 0.24	194.27	-18.98 ± 0.10	1.0	0.046	0.492	B
(480883) 2001 YE ₄	20.9	-69.87 ± 0.61	113.66	-50.95 ± 0.45	0.7	0.154 ^d	0.229*	-
(2340) Hathor	20.2	-29.94 ± 1.18	25.32	-17.34 ± 0.69	0.6	0.6	0.21	S
(483656) 2005 ES ₇₀	23.7	-140.17 ± 5.59	25.08	-80.11 ± 3.19	0.4	0.154 ^d	0.061*	-
(152563) 1992 BF [†]	19.7	-24.85 ± 1.17	21.17	-11.96 ± 0.56	0.3	0.287	0.272	Xc
2012 BB ₁₂₄	21.1	71.14 ± 4.05	17.58	29.42 ± 1.67	0.6	0.154 ^d	0.201*	-
(85990) 1999 JV ₆	20.2	-30.62 ± 2.19	13.98	-14.34 ± 1.03	0.6	0.095	0.451	Xk
(437844) 1999 MN	21.2	44.56 ± 4.26	10.46	41.35 ± 3.95	0.7	0.154 ^d	0.195*	S
(480808) 1994 XL ₁	20.8	-45.13 ± 4.35	10.38	-32.37 ± 3.12	0.5	0.154 ^d	0.237*	-
2007 TF ₆₈	22.7	-184.07 ± 17.91	10.28	-70.90 ± 6.90	0.8	0.154 ^d	0.099*	-
(1566) Icarus	16.3	-3.75 ± 0.39	9.73	-4.85 ± 0.50	0.4	0.14	1.44	S
(4179) Toutatis	15.2	-5.95 ± 0.65	9.20	-2.63 ± 0.29	1.1	0.13	2.45	S
(468468) 2004 KH ₁₇	21.9	-65.83 ± 8.08	8.15	-44.11 ± 5.41	0.6	0.072	0.197	C
(138175) 2000 EE ₁₀₄	20.3	-106.50 ± 11.89	8.95	-49.37 ± 5.51	1.4	0.154 ^d	0.297*	-
(1862) Apollo	16.1	-3.70 ± 0.42	8.76	-1.89 ± 0.22	0.4	0.26	1.4	Q
(2062) Aten	17.1	-13.18 ± 1.53	8.64	-5.89 ± 0.68	1.4	0.2	1.3	S
(162004) 1991 VE	18.1	26.97 ± 3.35	8.04	21.73 ± 2.70	1.0	0.154 ^d	0.824*	-
2006 TU ₇	21.9	166.67 ± 21.55	7.73	98.51 ± 12.74	1.0	0.154 ^d	0.141*	-
2011 PU ₁	25.5	-375.52 ± 49.66	7.56	-148.60 ± 19.65	0.4	0.154 ^d	0.027*	-
(6489) Golevka	19.0	-12.04 ± 1.67	7.21	-5.10 ± 0.71	0.5	0.151	0.53	Q
2011 EP ₅₁	25.3	-359.14 ± 51.20	7.01	-185.09 ± 26.39	0.5	0.154 ^d	0.029*	-
(33342) 1998 WT ₂₄	17.8	-27.87 ± 4.05	6.88	-16.91 ± 2.46	1.4	0.75	0.415	Xe
(3361) Orpheus	19.2	18.27 ± 2.70	6.77	7.88 ± 1.16	0.5	0.357	0.348	Q
(364136) 2006 CJ	20.1	-29.16 ± 4.52	6.46	-34.99 ± 5.42	0.4	0.154 ^d	0.317*	-
(499998) 2011 PT	24.0	-234.96 ± 37.16	6.32	-91.30 ± 14.44	0.5	0.154 ^d	0.053*	-
(138404) 2000 HA ₂₄	19.1	45.05 ± 7.15	6.30	19.95 ± 3.17	1.8	0.154 ^d	0.517*	S
2006 CT	22.3	-112.43 ± 18.09	6.22	-48.14 ± 7.74	0.6	0.154 ^d	0.119*	-
(3908) Nyx	17.3	25.45 ± 4.20	6.06	9.86 ± 1.63	1.4	0.23	1	V
(363599) 2004 FG ₁₁	21.0	-59.90 ± 10.17	5.89	-42.39 ± 7.20	0.8	0.306	0.152	V
1999 UQ	21.7	-110.45 ± 18.77	5.88	-44.85 ± 7.62	0.7	0.154 ^d	0.152*	-
2003 YL ₁₁₈	21.6	-172.62 ± 29.42	5.87	-90.31 ± 15.39	1.3	0.154 ^d	0.165*	-
(154590) 2003 MA ₃	21.6	-77.01 ± 13.11	5.87	-37.11 ± 6.32	0.3	0.530	0.086	-
2005 EY ₁₆₉	22.1	-137.02 ± 23.70	5.78	-53.80 ± 9.30	0.8	0.154 ^d	0.128*	-
(10302) 1989 ML	19.4	74.98 ± 13.09	5.73	28.76 ± 5.02	0.8	0.51	0.248	-
2000 PN ₈	22.1	123.75 ± 22.26	5.56	49.28 ± 8.87	0.7	0.154 ^d	0.131*	-
(506590) 2005 XB ₁	21.9	92.68 ± 17.54	5.28	44.88 ± 8.49	0.6	0.154 ^d	0.143*	-
(350462) 1998 KG ₃	22.1	-61.35 ± 11.79	5.21	-24.52 ± 4.71	0.3	0.154 ^d	0.129*	-
(216523) 2001 HY ₇	20.5	58.55 ± 11.23	5.21	31.33 ± 6.01	0.7	0.154 ^d	0.267*	-
(363505) 2003 UC ₂₀	18.3	-7.48 ± 1.44	5.20	-4.05 ± 0.78	0.7	0.028	1.9	C
(99907) 1989 VA	17.9	16.51 ± 3.19	5.18	12.71 ± 2.46	0.7	0.24	0.55	S
(66400) 1999 LT ₇	19.3	-43.09 ± 8.33	5.18	-29.44 ± 5.69	0.8	0.182	0.411	-
(377097) 2002 WQ ₄	19.5	-23.66 ± 4.61	5.13	-10.37 ± 2.02	0.4	0.154 ^d	0.423*	-
2000 CK ₅₉	24.2	-192.46 ± 37.77	5.10	-74.48 ± 14.62	0.4	0.154 ^d	0.05 *	-

Table 5: List of Yarkovsky detections with $3 \leq \text{SNR}_{A_2} < 5$ and with $\mathcal{S} \leq 2$. The table is sorted by SNR_{A_2} , in decreasing order. Columns and symbols are the same as in Table 4.

Asteroid	H	A_2 (10^{-15} au/d ²)	SNR_{A_2}	da/dt (10^{-4} au/My)	\mathcal{S}	p_v	D (km)	Tax. class
(29075) 1950 DA	17.1	-6.03 ± 1.25	4.83	-2.65 ± 0.55	0.5	0.07	2	-
(162117) 1998 SD ₁₅	19.1	-15.55 ± 3.28	4.74	-7.76 ± 1.64	0.6	0.154 ^d	0.51 *	S
2001 BB ₁₆	23.0	345.54 ± 73.84	4.68	163.59 ± 34.96	1.3	0.154 ^d	0.086*	-
(138852) 2000 WN ₁₀	20.1	36.04 ± 7.80	4.62	16.80 ± 3.64	0.5	0.154 ^d	0.316*	-
(455176) 1999 VF ₂₂	20.7	-69.25 ± 15.23	4.55	-56.46 ± 12.41	0.8	0.154 ^d	0.248*	-
(399308) 1993 GD	20.6	102.49 ± 22.73	4.51	43.94 ± 9.75	0.8	0.3	0.18	-
(7336) Saunders	18.8	39.34 ± 8.82	4.46	14.29 ± 3.20	1.7	0.18 †	0.553*	S
(1685) Toro	14.3	-3.76 ± 0.84	4.45	-1.68 ± 0.38	1.1	0.26	3.75	S
(4034) Vishnu	18.3	-66.24 ± 15.48	4.28	-34.03 ± 7.95	1.2	0.52	0.42	-
(85774) 1998 UT ₁₈	19.1	-6.64 ± 1.55	4.27	-2.67 ± 0.62	0.3	0.042	0.939	C
(310442) 2000 CH ₅₉	19.8	52.16 ± 12.25	4.26	29.04 ± 6.82	0.8	0.154 ^d	0.366*	-
(2100) Ra-Shalom	16.2	-4.65 ± 1.10	4.22	-2.67 ± 0.63	0.5	0.14	2.24	C
(326354) 2000 SJ ₃₄₄	22.8	-158.81 ± 37.77	4.20	-65.15 ± 15.49	0.7	0.154 ^d	0.093*	-
(481442) 2006 WO ₃	21.6	-62.26 ± 15.00	4.15	-36.97 ± 8.90	0.4	0.154 ^d	0.164*	-
(306383) 1993 VD	21.4	-29.85 ± 7.32	4.08	-19.46 ± 4.77	0.2	0.154 ^d	0.174*	-
(441987) 2010 NY ₆₅	21.5	-37.87 ± 9.28	4.08	-18.65 ± 4.57	0.4	0.071	0.228	C
2008 CE ₁₁₉	25.6	-143.47 ± 36.04	3.98	-57.16 ± 14.36	0.2	0.154 ^d	0.026*	-
(85953) 1999 FK ₂₁	18.1	-9.85 ± 2.49	3.95	-9.63 ± 2.44	0.5	0.32	0.59	S
(348306) 2005 AY ₂₈	21.6	-91.12 ± 23.12	3.94	-61.39 ± 15.58	0.7	0.154 ^d	0.166*	-
(65679) 1989 UQ	19.4	-37.59 ± 9.74	3.86	-17.95 ± 4.65	1.6	0.033	0.918	C
1995 CR	21.7	-85.94 ± 22.44	3.83	-155.89 ± 40.71	1.0	0.18 †	0.143*	S
(232691) 2004 AR ₁	19.8	-116.25 ± 30.33	3.83	-50.45 ± 13.16	1.9	0.154 ^d	0.369*	-
(265482) 2005 EE	21.2	93.97 ± 24.62	3.82	42.07 ± 11.02	0.8	0.154 ^d	0.197*	-
(136818) Selqet	19.0	24.44 ± 6.42	3.81	12.18 ± 3.20	0.6	0.15 †	0.548*	X
(425755) 2011 CP ₄	21.1	52.62 ± 13.99	3.76	96.46 ± 25.65	0.5	0.154 ^d	0.201*	-
(192559) 1998 VO	20.4	-33.01 ± 8.81	3.75	-14.25 ± 3.80	0.6	0.28	0.216	S
(163023) 2001 XU ₁	19.2	47.27 ± 12.70	3.72	32.04 ± 8.61	1.0	0.154 ^d	0.479*	-
(5604) 1992 FE	17.2	-24.03 ± 6.61	3.64	-12.68 ± 3.49	1.2	0.48	0.55	V
(397326) 2006 TC ₁	19.0	33.65 ± 9.23	3.65	12.68 ± 3.48	0.8	0.154 ^d	0.54 *	-
(208023) 1999 AQ ₁₀	20.4	-44.41 ± 12.21	3.64	-20.66 ± 5.68	1.0	0.154 ^d	0.281*	S
(437841) 1998 HD ₁₄	20.9	-87.22 ± 24.35	3.58	-41.83 ± 11.68	1.4	0.18 †	0.205*	Q
(413260) 2003 TL ₄	19.5	-36.09 ± 10.21	3.53	-20.36 ± 5.76	0.6	0.22	0.38	-
(4581) Asclepius	20.7	-40.76 ± 11.76	3.47	-19.62 ± 5.66	0.4	0.154 ^d	0.241*	-
(136582) 1992 BA	19.9	-54.38 ± 16.17	3.36	-20.03 ± 5.96	0.9	0.154 ^d	0.363*	-
(467351) 2003 KO ₂	20.4	97.34 ± 28.27	3.44	65.59 ± 19.05	1.2	0.154 ^d	0.277*	-
(7341) 1991 VK	16.8	-6.04 ± 1.84	3.29	-2.54 ± 0.77	0.6	0.18 †	1.344*	S
(256004) 2006 UP	23.0	-174.21 ± 53.10	3.28	-64.61 ± 19.69	0.6	0.154 ^d	0.084*	-
(450300) 2004 QD ₁₄	20.6	-116.65 ± 35.73	3.26	-57.61 ± 17.65	1.4	0.154 ^d	0.263*	-
(477719) 2010 SG ₁₅	25.2	-237.31 ± 74.49	3.19	-90.57 ± 28.43	0.3	0.154 ^d	0.031*	-
(37655) Illapa	17.8	-13.41 ± 4.26	3.15	-10.81 ± 3.43	0.6	0.154 ^d	0.938*	-
(267759) 2003 MC ₇	18.7	-29.24 ± 9.36	3.12	-10.97 ± 3.51	0.8	0.154 ^d	0.611*	-
(310842) 2003 AK ₁₈	19.7	-33.50 ± 10.94	3.06	-17.83 ± 5.82	0.6	0.154 ^d	0.385*	-
(162783) 2000 YJ ₁₁	20.6	-127.26 ± 42.13	3.02	-49.85 ± 16.50	1.4	0.154 ^d	0.257*	-
(152671) 1998 HL ₃	20.1	-55.64 ± 18.40	3.02	-25.68 ± 8.49	0.7	0.2	0.298	-

Table 6: List of rejected Yarkovsky detections. The table is sorted by SNR_{A_2} , in decreasing order. The columns are the same as in Table 4, but the one showing da/dt .

Asteroid	H	A_2 (10^{-15} au/d ²)		SNR_{A_2}	S	p_v	D (km)	Tax. class
(4015) Wilson-Harrington	16.0	-16.48	± 7.16	2.30	2.9	0.046	3.821	C
(260141) 2004 QT ₂₄	18.3	530.90	± 53.46	9.93	20.8	0.42	0.454*	S
(350751) 2002 AW	20.7	-579.13	± 116.36	4.98	6.5	0.154 ^d	0.243*	B
(39565) 1992 SL	18.4	-100.52	± 20.41	4.92	3.1	0.154 ^d	0.698*	-
(4486) Mithra	15.4	-83.37	± 18.47	4.51	12.9	0.297	1.849	V
(474158) 1999 FA	20.6	-93.01	± 22.25	4.18	1.7	0.18 †	0.233*	S
(162421) 2000 ET ₇₀	18.0	-33.73	± 10.80	3.12	3.4	0.15 †	2.26	-
(308635) 2005 YU ₅₅	21.6	-317.23	± 60.43	5.25	4.5	0.065	0.306	C
(139359) 2001 ME ₁	16.6	-307.68	± 60.74	5.07	45.0	0.04	3.15 *	C
(433) Eros	10.8	-1.96	± 0.40	4.96	2.7	0.25	16.84	S
(175706) 1996 FG ₃	18.3	-55.77	± 12.90	4.32	3.1	0.072	1.196	C
2010 KP ₁₀	23.4	2981.28	± 915.15	3.26	11.4	0.101	0.087	-
(142561) 2002 TX ₆₈	18.1	-466.98	± 153.85	3.04	35.3	0.154 ^d	0.801*	Xe
(192563) 1998 WZ ₆	17.3	-54.76	± 18.17	3.01	3.7	0.30	0.8	V

Table 7: List of marginal significance detections, which means $2.5 < \text{SNR}_{A_2} < 3$ and $S \leq 2$. The table is sorted by SNR_{A_2} , in decreasing order (apart from the two special cases at the top). Columns and symbols are the same as in Table 4.

Asteroid	H	A_2 (10^{-15} au/d ²)		SNR_{A_2}	da/dt (10^{-4} au/My)		S	p_v	D (km)	Tax. class
(99942) Apophis	18.9	-53.39	± 29.60	1.80	-24.50	± 13.58	1.6	0.30	0.375	S
(410777) 2009 FD	22.1	21.49	± 47.40	0.45	11.18	± 24.66	0.4	0.01	0.472	-
(162080) 1998 DG ₁₆	19.8	-37.93	± 12.84	2.95	-19.51	± 6.61	1.4	0.035	0.777	C
(85770) 1998 UP ₁	20.4	-34.77	± 11.84	2.94	-16.77	± 5.71	0.8	0.154 ^d	0.282*	S
(162142) 1998 VR	18.7	17.59	± 5.98	2.94	8.88	± 3.02	0.8	0.18 †	0.6	S
2002 LY ₁	22.4	-166.14	± 57.73	2.88	-84.31	± 29.30	0.8	0.154 ^d	0.114*	-
(474163) 1999 SO ₅	20.9	-79.89	± 27.78	2.88	-32.69	± 11.37	0.8	0.154 ^d	0.22 *	-
(242191) 2003 NZ ₆	19.0	38.23	± 13.29	2.88	24.07	± 8.37	0.6	0.334	0.370	-
(215588) 2003 HF ₂	19.4	-79.07	± 27.60	2.87	-58.53	± 20.43	1.7	0.118	0.488	-
(162181) 1999 LF ₆	18.2	-22.41	± 7.86	2.85	-8.70	± 3.05	1.3	0.175	0.729	S
(164207) 2004 GU ₉	21.1	-69.93	± 24.83	2.82	-30.24	± 10.74	0.5	0.219	0.163	-
2001 QC ₃₄	20.1	-73.87	± 26.33	2.81	-30.61	± 10.91	1.9	0.154 ^d	0.329*	Q
(283457) 2001 MQ ₃	18.9	-38.45	± 13.73	2.80	-13.80	± 4.93	0.9	0.154 ^d	0.56 *	-
2007 PB ₈	21.2	-160.83	± 58.50	2.75	-90.77	± 33.01	1.4	0.154 ^d	0.198*	-
(230111) 2001 BE ₁₀	19.2	-28.81	± 10.72	2.69	-15.61	± 5.81	0.9	0.253	0.4	S
1999 SK ₁₀	19.7	-45.84	± 17.24	2.66	-18.21	± 6.85	1.0	0.346	0.259	S
(338292) 2002 UA ₃₁	19.0	-35.78	± 13.48	2.65	-22.29	± 8.40	0.8	0.154 ^d	0.538*	-
(334412) 2002 EZ ₂	20.1	-119.39	± 45.75	2.61	-45.46	± 17.42	1.1	0.40	0.21	-
(376879) 2001 WW ₁	22.0	-63.88	± 24.83	2.57	-25.03	± 9.73	0.4	0.154 ^d	0.135*	-
(416151) 2002 RQ ₂₅	20.6	55.10	± 21.64	2.55	24.49	± 9.62	0.7	0.154 ^d	0.262*	C
(503941) 2003 UV ₁₁	19.5	6.66	± 2.63	2.53	5.62	± 2.22	0.1	0.376	0.26	Q
(471240) 2011 BT ₁₅	21.7	-196.07	± 77.53	2.53	-80.55	± 31.85	1.3	0.154 ^d	0.154*	-
1994 CJ ₁	21.5	-138.42	± 55.12	2.51	-53.87	± 21.45	1.0	0.154 ^d	0.167*	-
(54509) YORP	22.6	-74.61	± 29.88	2.50	-33.45	± 13.40	0.6	0.154 ^d	0.1	S

Table 8: List of detections including both the Yarkovsky effect and solar radiation pressure, that is the set of asteroids for which the parameter A_1 was reliably determined with a signal-to-noise ratio $\text{SNR}_{A_1} > 3$.

Asteroid	A_2 (10^{-15} au/d ²)		SNR_{A_2}	S	A_1 (10^{-15} au/d ²)		SNR_{A_1}	A/M (m ² /ton)	D (m)		
2009 BD	-1152	±	82	14.0	0.2	57 663	±	8674	6.7	0.3	4
2012 LA	-4907	±	12 832	0.4	2.2	81 216	±	16 312	5.0	0.4	10*
2011 MD	-2006	±	3049	0.7	0.5	75 074	±	24 396	3.1	0.3	6
2015 TC ₂₅	-4433	±	2754	1.6	1.4	160 079	±	20 065	8.0	0.7	3*
2006 RH ₁₂₀	-50 469	±	3787	13.3	9.0	124 099	±	4747	26.1	0.6	4*

Table 9: Comparison between the accepted results of this paper ($\text{SNR}_{A_2} \geq 5$) and the JPL ones. The columns contain the asteroid name, the signal-to-noise ratio of our solution and of the JPL one, the ratio $\sigma_{A_2, \text{JPL}}/\sigma_{A_2}$ of the A_2 uncertainties as estimated by the two systems, the relative errors computed with our A_2 uncertainty and with the JPL A_2 uncertainty respectively, and the χ_{A_2} value.

Asteroid	SNR_{A_2}	$\text{SNR}_{A_2}^{\text{JPL}}$	$\sigma_{A_2, \text{JPL}}/\sigma_{A_2}$	$\varepsilon_r(A_2)$	$\varepsilon_r^{\text{JPL}}(A_2)$	χ_{A_2}
(101955) Benu	192.50	182.10	1.06	0.23	0.22	0.173
(480883) 2001 YE ₄	114.54	72.38	1.58	0.29	0.18	0.149
(2340) Hathor	25.37	24.29	1.06	0.29	0.28	0.204
(483656) 2005 ES ₇₀	25.08	18.39	1.39	0.40	0.29	0.236
(152563) 1992 BF	21.24	27.49	0.81	1.05	1.30	0.816
2012 BB ₁₂₄	17.57	9.00	1.86	0.83	0.45	0.392
(85990) 1999 JV ₆	13.98	12.58	1.22	1.37	1.12	0.869
(437844) 1999 MN	10.46	8.42	1.17	0.59	0.50	0.381
(480808) 1994 XL ₁	10.37	11.81	0.93	0.61	0.66	0.446
2007 TF ₆₈	10.28	6.02	1.55	0.95	0.62	0.517
(1566) Icarus	9.62	3.79	2.10	1.64	0.78	0.705
(138175) 2000 EE ₁₀₄	8.96	6.86	1.20	0.72	0.60	0.460
(1862) Apollo	8.81	7.23	1.12	0.71	0.63	0.476
(2062) Aten	8.61	7.34	1.07	0.79	0.74	0.541
(468468) 2004 KH ₁₇	8.15	6.55	1.28	0.27	0.21	0.167
(162004) 1991 VE	8.05	6.10	1.14	1.07	0.93	0.704
2006 TU ₇	7.73	5.58	1.40	0.08	0.06	0.045
2011 PU ₁	7.56	6.00	1.01	1.52	1.51	1.074
(6489) Golevka	7.21	7.91	0.87	0.32	0.36	0.239
2011 EP ₅₁	7.01	6.46	0.98	0.71	0.72	0.505
(33342) 1998 WT ₂₄	6.88	5.27	1.22	0.43	0.35	0.273
(3361) Orpheus	6.77	7.10	1.09	0.99	0.91	0.668
(364136) 2006 CJ	6.45	8.26	0.74	0.32	0.44	0.261
(499998) 2011 PT	6.32	7.40	0.81	0.30	0.37	0.236
(138404) 2000 HA ₂₄	6.30	2.05	2.82	0.53	0.19	0.177
2006 CT	6.22	5.82	0.99	0.45	0.45	0.319
(3908) Nyx	6.06	4.62	1.29	0.08	0.06	0.047
(363599) 2004 FG ₁₁	5.89	3.81	1.56	0.05	0.03	0.027
1999 UQ	5.88	3.39	1.87	0.43	0.23	0.205
2003 YL ₁₁₈	5.87	4.71	1.18	0.32	0.28	0.210
(154590) 2003 MA ₃	5.87	4.75	1.19	0.25	0.21	0.159
2005 EY ₁₆₉	5.78	4.29	1.22	0.57	0.47	0.360
(10302) 1989 ML	5.73	4.58	1.02	1.06	1.03	0.738
2000 PN ₈	5.56	5.43	1.07	0.25	0.23	0.172
(506590) 2005 XB ₁	5.28	5.59	1.09	0.78	0.72	0.531
(216523) 2001 HY ₇	5.21	4.52	1.09	0.29	0.27	0.198
(350462) 1998 KG ₃	5.20	5.75	0.89	0.11	0.12	0.079
(363505) 2003 UC ₂₀	5.19	2.57	1.22	2.06	1.68	1.302
(99907) 1989 VA	5.18	3.63	1.30	0.45	0.34	0.273
(66400) 1999 LT ₇	5.17	4.37	1.20	0.06	0.05	0.037
(377097) 2002 WQ ₄	5.13	3.93	1.32	0.05	0.04	0.029
2000 CK ₅₉	5.10	5.76	0.87	0.10	0.11	0.074

Table 10: Comparison between the accepted results of this paper ($\text{SNR}_{A_2} < 5$) and the JPL ones. The columns are the same of Table 9.

Asteroid	SNR_{A_2}	$\text{SNR}_{A_2}^{\text{JPL}}$	$\sigma_{A_2, \text{JPL}}/\sigma_{A_2}$	$\varepsilon_r(A_2)$	$\varepsilon_r^{\text{JPL}}(A_2)$	χ_{A_2}
(29075) 1950 DA	4.82	4.17	1.03	0.51	0.49	0.351
(162117) 1998 SD ₁₅	4.74	4.35	1.23	0.62	0.51	0.394
2001 BB ₁₆	4.68	4.86	1.14	0.86	0.75	0.567
(138852) 2000 WN ₁₀	4.62	4.29	1.04	0.17	0.16	0.116
(455176) 1999 VF ₂₂	4.55	3.99	1.27	0.51	0.40	0.313
(399308) 1993 GD	4.51	4.45	0.98	0.17	0.17	0.120
(1685) Toro	4.48	4.33	0.85	0.81	0.95	0.618
(7336) Saunders	4.46	2.76	1.22	1.08	0.89	0.686
(4034) Vishnu	4.28	4.31	1.15	0.66	0.57	0.433
(85774) 1998 UT ₁₈	4.28	3.44	1.11	0.48	0.44	0.325
(310442) 2000 CH ₅₉	4.26	2.60	1.38	0.68	0.50	0.402
(2100) Ra-Shalom	4.23	3.10	1.14	0.69	0.61	0.456
(326354) 2000 SJ ₃₄₄	4.20	6.92	0.65	0.28	0.44	0.237
(481442) 2006 WO ₃	4.15	3.97	0.94	0.41	0.44	0.300
(441987) 2010 NY ₆₅	4.08	3.88	1.03	0.07	0.07	0.047
(306383) 1993 VD	4.08	1.61	1.35	1.91	1.42	1.137
2008 CE ₁₁₉	3.98	3.43	1.57	1.41	0.90	0.756
(85953) 1999 FK ₂₁	3.96	4.94	0.89	0.44	0.49	0.327
(348306) 2005 AY ₂₈	3.94	4.23	0.75	0.76	1.01	0.606
(65679) 1989 UQ	3.86	3.74	1.07	0.14	0.13	0.097
(232691) 2004 AR ₁	3.83	2.28	1.08	1.38	1.29	0.942
1995 CR	3.83	2.23	1.42	0.65	0.46	0.374
(265482) 2005 EE	3.82	1.58	1.48	1.46	0.99	0.818
(136818) Selqet	3.81	2.08	1.37	0.96	0.70	0.566
(425755) 2011 CP ₄	3.76	3.37	1.24	0.40	0.33	0.254
(192559) 1998 VO	3.75	3.77	0.92	0.26	0.29	0.194
(163023) 2001 XU ₁	3.72	2.94	1.05	0.63	0.60	0.432
(397326) 2006 TC ₁	3.65	3.45	0.98	0.26	0.27	0.188
(208023) 1999 AQ ₁₀	3.64	2.27	1.14	1.05	0.93	0.696
(5604) 1992 FE	3.64	3.46	1.24	0.64	0.52	0.402
(437841) 1998 HD ₁₄	3.58	3.26	0.87	0.73	0.84	0.551
(413260) 2003 TL ₄	3.53	2.85	1.02	0.61	0.60	0.429
(4581) Asclepius	3.47	2.57	1.20	0.39	0.32	0.247
(467351) 2003 KO ₂	3.44	2.93	1.34	0.49	0.37	0.294
(136582) 1992 BA	3.36	3.43	1.18	0.70	0.59	0.449
(256004) 2006 UP	3.28	3.65	0.95	0.18	0.19	0.133
(7341) 1991 VK	3.28	3.72	1.07	0.68	0.64	0.465
(450300) 2004 QD ₁₄	3.26	1.99	2.03	0.78	0.38	0.342
(477719) 2010 SG ₁₅	3.19	2.78	1.01	0.39	0.38	0.272
(37655) Illapa	3.15	2.67	1.14	0.10	0.09	0.065
(267759) 2003 MC ₇	3.12	3.57	0.87	0.01	0.02	0.010
(310842) 2003 AK ₁₈	3.06	2.60	1.31	0.35	0.27	0.214
(162783) 2000 YJ ₁₁	3.02	3.38	0.94	0.16	0.17	0.114
(152671) 1998 HL ₃	3.02	3.16	0.98	0.06	0.06	0.042
(85770) 1998 UP ₁	2.94	3.01	1.42	1.34	0.94	0.771
(474163) 1999 SO ₅	2.88	3.51	1.02	0.72	0.70	0.501
(283457) 2001 MQ ₃	2.80	3.91	0.87	0.61	0.70	0.462
(376879) 2001 WW ₁	2.57	3.07	0.76	0.24	0.31	0.188
(99942) Apophis	1.80	2.54	0.74	0.09	0.12	0.069
(410777) 2009 FD	0.45	0.04	1.22	0.51	0.42	0.321

*

Table 11: Results of the comparison between the estimated values of A_2 and A_1 , as contained in this paper and in the JPL database. In particular, the columns contain the asteroid name, the signal-to-noise ratio of our A_2 solution and of the JPL one, the signal-to-noise ratio of our A_1 solution and of the JPL one, the relative error in the A_2 parameter computed with our A_2 uncertainty and with the JPL A_2 uncertainty respectively, the relative error in the A_1 parameter computed with our A_1 uncertainty and with the JPL A_1 uncertainty respectively, the χ -value for A_2 and for A_1 .

Asteroid	SNR_{A_2}	$\text{SNR}_{A_2}^{\text{JPL}}$	SNR_{A_1}	$\text{SNR}_{A_1}^{\text{JPL}}$	$\varepsilon_r(A_2)$	$\varepsilon_r^{\text{JPL}}(A_2)$	$\varepsilon_r(A_1)$	$\varepsilon_r^{\text{JPL}}(A_1)$	χ_{A_2}	χ_{A_1}
2009 BD	14.0	13.9	6.7	6.3	0.12	0.12	0.44	0.45	0.084	0.315
2012 LA	0.4	0.3	5.0	6.9	0.22	0.37	0.04	0.05	0.189	0.029
2011 MD	0.7	0.3	3.1	3.1	0.32	0.25	0.11	0.10	0.198	0.074
2015 TC ₂₅	1.6	1.6	8.0	7.6	0.06	0.05	0.11	0.11	0.039	0.076
2006 RH ₁₂₀	13.3	11.1	26.1	23.4	0.16	0.13	1.62	1.36	0.100	1.043

Table 12: Impact monitoring of asteroid 2001 BB₁₆ with a non-gravitational model that includes the Yarkovsky effect. Table columns: calendar date (year, month, and day) for the potential impact for asteroid 2011 MD, approximate σ value of the virtual impactor location along the LOV, minimum distance (the lateral distance from the LOV to the center of the Earth on the TP confidence region), stretching (how much the confidence region at the epoch has been stretched by the time of impact), probability of Earth impact (IP), and Palermo Scale (PS). The width of the TP confidence region is always few km, thus not reported.

Date	σ	Distance (R_\oplus)	Stretching (R_\oplus)	IP	PS
2195/01/15.525	-3.404	3.17	$5.20 \cdot 10^3$	$2.91 \cdot 10^{-7}$	-6.35
2199/01/15.844	-3.164	2.10	$8.36 \cdot 10^4$	$5.02 \cdot 10^{-8}$	-7.12

Table 13: Impact monitoring of asteroid 2011 MD with a non-gravitational model that includes both the Yarkovsky effect and solar radiation pressure. Columns as in Table 12.

Date	σ	Distance (R_{\oplus})	Stretching (R_{\oplus})	IP	PS
2083/06/13.856	2.720	6.44	$2.86 \cdot 10^4$	$3.54 \cdot 10^{-7}$	-8.29
2098/06/07.618	0.428	6.38	$9.00 \cdot 10^5$	$4.33 \cdot 10^{-7}$	-8.29
2099/06/08.786	0.370	5.68	$3.70 \cdot 10^5$	$1.32 \cdot 10^{-6}$	-7.81
2102/06/13.699	-0.250	6.40	$5.23 \cdot 10^4$	$7.61 \cdot 10^{-6}$	-7.06
2110/05/28.604	-0.993	5.52	$1.48 \cdot 10^6$	$2.09 \cdot 10^{-7}$	-8.66
2113/06/09.765	0.330	4.09	$9.48 \cdot 10^5$	$6.90 \cdot 10^{-7}$	-8.15
2116/06/08.850	0.258	6.37	$2.61 \cdot 10^6$	$1.57 \cdot 10^{-7}$	-8.81
2116/06/08.870	0.258	6.24	$3.78 \cdot 10^6$	$1.14 \cdot 10^{-7}$	-8.95
2118/06/07.317	0.472	6.12	$1.52 \cdot 10^6$	$2.65 \cdot 10^{-7}$	-8.59
2118/06/10.605	1.496	4.80	$3.54 \cdot 10^5$	$5.66 \cdot 10^{-7}$	-8.26
2119/06/14.086	-0.670	6.55	$3.30 \cdot 10^4$	$9.22 \cdot 10^{-6}$	-7.05
2119/06/14.181	-0.670	1.70	$9.79 \cdot 10^5$	$6.57 \cdot 10^{-7}$	-8.20
2120/06/04.434	0.520	5.51	$3.44 \cdot 10^6$	$1.69 \cdot 10^{-7}$	-8.79
2122/06/11.859	1.223	5.48	$1.25 \cdot 10^6$	$2.07 \cdot 10^{-7}$	-8.72
2123/06/08.803	0.416	4.78	$1.28 \cdot 10^6$	$4.34 \cdot 10^{-7}$	-8.40
2132/06/09.046	0.184	6.30	$3.78 \cdot 10^6$	$1.13 \cdot 10^{-7}$	-9.02
2137/06/11.124	1.218	6.18	$2.09 \cdot 10^6$	$1.01 \cdot 10^{-7}$	-9.08
2139/06/12.675	1.240	5.83	$8.80 \cdot 10^5$	$2.58 \cdot 10^{-7}$	-8.68
2140/06/12.052	1.301	4.52	$7.04 \cdot 10^5$	$3.98 \cdot 10^{-7}$	-8.50
2151/06/12.350	-0.796	6.93	$1.66 \cdot 10^6$	$1.20 \cdot 10^{-7}$	-9.05
2151/06/12.604	-0.732	6.44	$2.90 \cdot 10^6$	$1.05 \cdot 10^{-7}$	-9.11
2151/06/12.780	-0.762	2.96	$3.16 \cdot 10^6$	$1.76 \cdot 10^{-7}$	-8.89
2155/06/11.940	-0.439	6.54	$5.27 \cdot 10^4$	$5.87 \cdot 10^{-6}$	-7.37
2155/06/11.984	-0.436	2.86	$2.98 \cdot 10^5$	$2.29 \cdot 10^{-6}$	-7.78
2155/06/12.054	-0.439	2.92	$8.38 \cdot 10^4$	$8.04 \cdot 10^{-6}$	-7.24
2155/06/12.168	-0.437	7.06	$1.96 \cdot 10^4$	$1.44 \cdot 10^{-5}$	-6.98
2158/06/11.842	-2.091	7.19	$2.80 \cdot 10^5$	$1.19 \cdot 10^{-7}$	-9.08
2182/06/09.849	0.041	4.51	$5.95 \cdot 10^6$	$1.09 \cdot 10^{-7}$	-9.18

Table 14: Impact monitoring of asteroid 2011 MD with a non-gravitational model including solar radiation pressure only. Columns as in Table 12.

Date	σ	Distance (R_{\oplus})	Stretching (R_{\oplus})	IP	PS
2133/12/05.197	-0.476	0.27	$1.98 \cdot 10^6$	$3.58 \cdot 10^{-7}$	-8.52
2140/11/25.578	-0.352	4.66	$5.53 \cdot 10^6$	$1.12 \cdot 10^{-7}$	-9.05
2147/11/27.042	0.212	4.79	$1.17 \cdot 10^5$	$5.13 \cdot 10^{-6}$	-7.41
2168/05/22.293	0.081	4.70	$2.13 \cdot 10^6$	$2.87 \cdot 10^{-7}$	-8.72
2169/11/26.849	-0.053	5.48	$1.92 \cdot 10^6$	$2.76 \cdot 10^{-7}$	-8.74
2186/11/21.935	-0.633	6.87	$1.56 \cdot 10^6$	$1.46 \cdot 10^{-7}$	-9.06